Theoretical and Applied Climatology
https://doi.org/10.1007/s00704-024-04995-7

RESEARCH

Modelling the potential of land use change to mitigate the impacts of climate change on future drought in the Western Cape, South Africa

Myra Naik[1] · **Babatunde J. Abiodun**[1,2]

Received: 6 January 2024 / Accepted: 28 April 2024

Abstract

Several studies have shown that climate change may enhance the severity of droughts over the Western Cape (South Africa) in the future, but there is a dearth of information on how to reduce the impacts of climate change on water yields. This study investigates the extent to which land-use changes can reduce the projected impacts of climate change on hydrological droughts in the Western Cape catchments. For the study, the Soil Water Assessment Tool (SWAT+) model was calibrated and evaluated over several river catchments, and the climate simulation dataset from the COordinated Regional Downscaling EXperiment (CORDEX) was bias-corrected. Using the bias-corrected climate data as a forcing, the SWAT+ was used to project the impacts of future climate change on water yield in the catchments and to quantify the sensitivity of the projection to four feasible land-use change scenarios in the catchments. The land-use scenarios are the spread of forest (FOMI), the restoration of shrubland (SHRB), the expansion of cropland (CRDY), and the restoration of grassland (GRSL).

The model evaluation shows a good agreement between the simulated and observed monthly streamflows at four stations, and the bias correction of the CORDEX dataset improved the hydrological simulations. The climate change projection features an increase in temperature and potential evaporation, but a decrease in precipitation and all the hydrological variables. The drying occurs across the Western Cape, with the magnitude increasing with higher global warming levels (GWLs). The land-use changes alter these climate change impacts through changes in the hydrological water balance. FOMI increases streamflow and decreases runoff, while SHRB decreases streamflow and runoff. The influence of CRDY and GRSL are more complex. However, all the impacts of land-use changes are negligible compared to the impacts of climate change. Hence, land-use changes in the Western Cape may not be the most efficient strategies for mitigating the impacts of climate change on hydrological droughts over the region. The results of the study have application towards improving water security in the Western Cape river catchments.

1 Introduction

The Western Cape Province (in South Africa) is a water-scarce region. The region experienced one of its worst multi-year droughts in 2015–2017, when a meteorological drought cascaded to agricultural, hydrological, and socio-economic impacts. During this extended drought, the water storage levels of the Western Cape's major dams deteriorated to about 23%; meanwhile, the last 12% of the dam water was unusable (Botai et al. 2017). The province was declared a disaster region, and the crisis triggered the local government to impose severe water restrictions on agricultural, urban, and industrial consumers, while exploring strategies to avert a situation where the taps ran completely dry. The drought had a significant impact on agriculture, livelihoods, and communities. For instance, the agricultural sector suffered economic losses estimated at ZAR 5.9 billion, and at least 30 000 jobs were lost (Green Cape 2019). Moreover, the Western Cape is likely to become drier, and to experience moderate to strong warming in the near future (*e.g.,* Field et al. 2014; Midgley et al. 2007). By 2050, it is projected that Western Cape rainfall may decrease by about 30% from current levels (Roux 2018). Such reductions in rainfall may impact dam levels and surface water budgets, with serious implications for agriculture and industry. Some climate

✉ Myra Naik
myranaik@gmail.com

1 Climate System Analysis Group, Department of Environmental and Geographical Science, University of Cape Town, Cape Town, South Africa

2 Nansen-Tutu Centre for Marine Environmental Research, Department Oceanography, University of Cape Town, Cape Town, South Africa

projections already suggest that future drought across the region may be more severe and more frequent (see Naik and Abiodun 2020). Thus, along with rising temperatures and increasing evaporation, the implications of drought and climate change for long-term water security may be serious. The need to minimize future drought impacts on water availability in the province has necessitated studies on mitigating the impacts of climate change on droughts.

Land-use and land-cover (LULC) changes play a crucial role in influencing the hydrology of a basin. They may have positive or negative impacts on water cycle and water yield in the basin by influencing processes like evapotranspiration, vegetation interception, and surface infiltration (Guo et al. 2014). However, the magnitude and direction of these hydrological impacts depend on the type and extent of the land-use change (Lumsden and Schulze 2003). For instance, forestation may reduce soil moisture and surface runoff, while urbanization and human settlement may give rise to higher storm flow and enhanced discharge peaks. Jia et al. (2017) showed that removal of forest reduced the soil moisture across the Loess Plateau (in China). Farley et al. (2005) reported reductions in runoff following the forestation of grassland/shrubland and indicated that the reduction may be higher in drier regions. Youpeng et al. (2010) found that the expansion of urban areas increased surface runoff over the Yangtze River Delta, China. Holder et al. (2019) also showed that conversion of temperate grassland to crops in the western United Kingdom decreased surface runoff. To date, however, only few empirical studies (e.g., Albhaisi et al. 2013; Gyamfi et al. 2016a; Schütte & Schulze 2017; Warburton et al. 2012) have modelled LULC changes impacts on hydrological processes over South Africa, and there remains a dearth of information on how LULC changes may influence future hydrological drought in the Western Cape river catchments.

Some studies have speculated that removal of invasive alien vegetation from the Western Cape river catchments may reduce the severity of hydrological droughts. This is because the invasive alien vegetation reduces runoff into the major dams that supply the Western Cape Water Supply System. Some estimates suggest that more than 100 million litres per day (about 20% of Cape Town's water requirement) are lost due to invasive alien vegetation in these catchments (Ground Up 2018). Hence, there is some consensus (*e.g.,* Le Maitre et al. 2016, 2019; Rostorfer et al. 2015; Turpie 2018) that the removal of invasive alien vegetation often found in old forestry plantations surrounding these river catchments (*e.g.*, Steenbras, Berg and Theewaterskloof) may increase surface water flows, and thereby offer an economically cheap and environmentally low risk option to improve water security for the greater Cape Town area. Indeed, it may even be that removal of alien vegetation may also reduce the severity of hydrological drought due to future climate change. Catchment rehabilitation studies that re-establish and protect natural vegetation (after clearance of invasive alien vegetation) may prove beneficial both from an economic and water security perspective (e.g., Le Maitre et al. 2019; Rostorfer et al. 2015; Turpie 2018). Previous research by Tizora et al. (2016) examined historical land-use in the Western Cape Province and found that there has been a decrease in forest plantations, grasslands, wetlands, and barren lands over recent years, but also increases in urbanization, mines and quarries, water bodies, woodlands, thicket and shrubland. While a previous study in the region also assessed the potential impacts of future drought in river catchments (Naik and Abiodun 2020), there remains a dearth of information on how land-use change may influence the risk of future hydrological droughts in the Western Cape.

For this study we used the Soil and Water Assessment Tool Plus (SWAT +), the new generation of the SWAT–a public domain model, jointly developed by the USDA Agricultural Research Service (USDA-ARS) and Texas A&M AgriLife Research (Arnold, et al. 1998; 2012). SWAT is widely used, for example, in assessing soil erosion prevention and control, non-point source pollution control and regional management in watersheds (Krysanova and White 2015; Tan et al. 2019; van Griensven et al. 2012). SWAT is suitable for hydrological modelling streamflow conditions over the South African domain (Andersson et al. 2011; Mengistu et al. 2019; Scott-Shaw et al. 2020; Thavhana et al. 2018) and has been applied and calibrated over South African catchments (e.g., Gyamfi et al. 2016a; Ncube and Taigbenu 2005), as well as extensively used for studying the impact of land-use changes. However, there remains limited application of SWAT + to examine on how LULC changes may influence future hydrological drought. The aim of the present study is to investigate the extent to which some land-use changes can mitigate the impact of future droughts in the Western Cape river catchments. This study is structured as follows: Section. 2 describes the data and methods used in the study, Section. 3 presents the results and discussion, and Section. 4 gives the conclusions of the study.

2 Methodology

2.1 Study region

The Western Cape Province (about 30°S–35°S; 17°E–25°E) is located in the southernmost part of Southern Africa (Fig. 1a). The economic activities in the province include manufacturing, construction, mining, and agriculture. The Mediterranean climate of the region offers warm dry summers (reaching about 15 to 27 °C) and cold winters (about 5 to 22 °C), but highly variable rainfall. The Western Cape is one of South Africa's driest regions, with only 350 mm

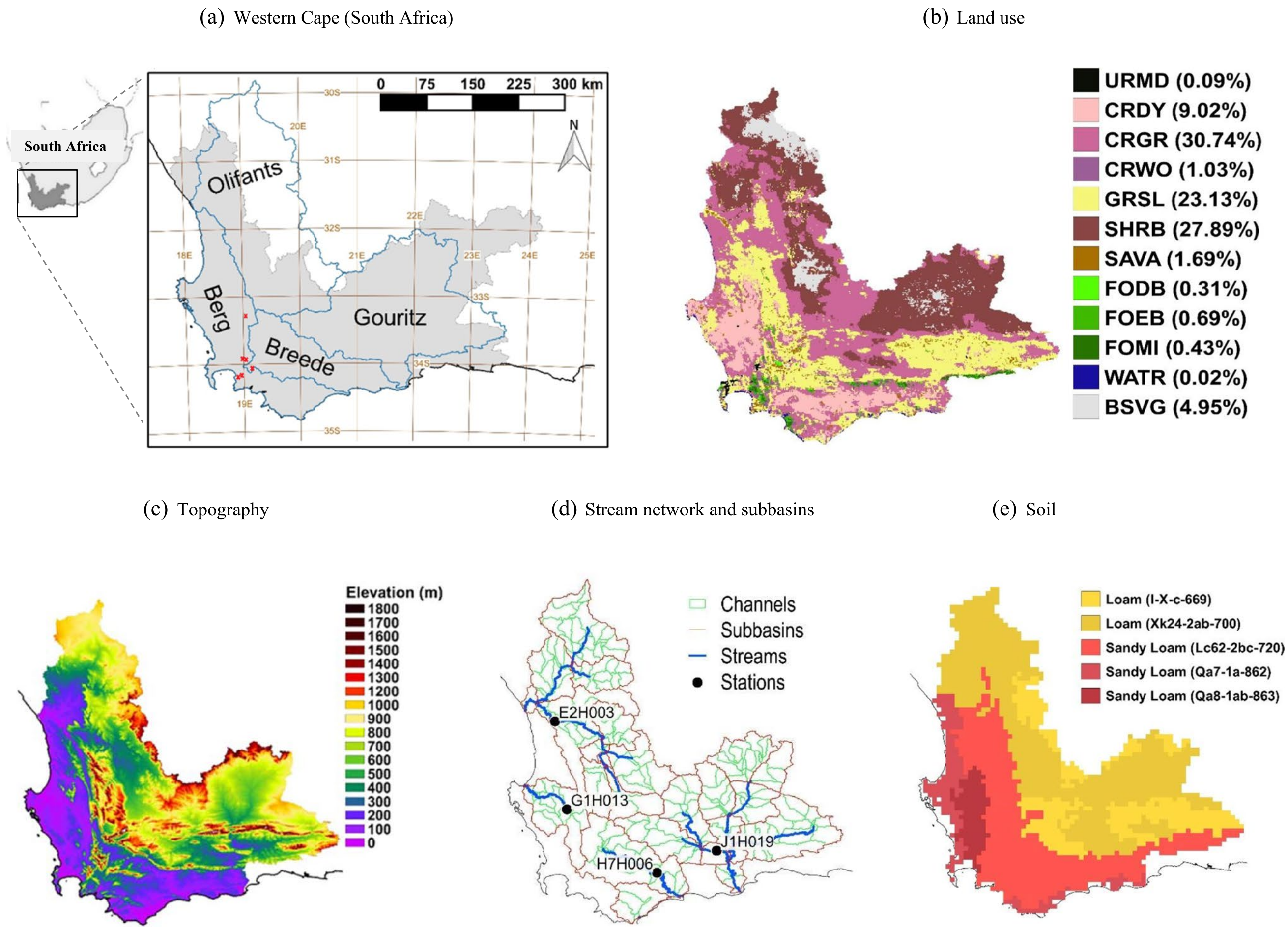

Fig. 1 The characteristics of the Western Cape catchments as used in the study: (**a**) the four river catchments (Berg, Breede, Olifants and Gouritz, with red dots to indicate major dams); (**b**) land-use (the percentage of each land-cover type is indicated in brackets); (**c**) topography (Digital Elevation Model); (**d**) the SWAT+delineations of the catchments: streams (with streamflow observation stations), subbasin and channels; and (**e**) soil types

of rain per year, far less than the national annual average of 500 mm (Dennis & Dennis, 2012). In contrast to much of southern Africa, which experiences summer rains and dry winters, the Western Cape is unique in that it receives its highest precipitation during the austral winter months of June-July–August (JJA). Rainfall is, however, highly heterogeneous, varying considerably with the region's complex topography (Fig. 1c). Mean annual rainfall varies significantly, with mountainous regions receiving up to 3000 mm of rain, while low-lying regions (40 m above sea level) receive less than 200 mm (Lakhraj-Govender & Grab 2019). The prominent Cape Fold Mountain Belt extends along the length of the province (1300 km), forming an L-shaped mountain range that extends north–south, along the western coast, and east–west along the southern coast. This mountain range acts as an orographic barrier that creates dry interior conditions and augments the rainfall (through orographic rain) in the coastal parts. The Western Cape Province has three major rainfall zones, including the winter, late summer, and all-year seasonality regimes. The winter rainfall zone occurs along the south-western and western parts of the province (West Coast), where annual precipitation ranges from less than 200 mm (in the north) to over 1000 mm (over the mountainous regions). This zone typically receives winter rainfall (May to August) from mid-latitude cyclones originating over the South Atlantic, and it is affected by the combination of the cold Benguela current and the northward displacement of high-pressure systems (Du Plessis & Scholms 2017). The late summer (February–March) rainfall zone occurs over the north-east part of the province (Great Karoo) and is bound inland by South Africa's interior plateau. The all-year rainfall zone occurs along the southern coastline, stretching eastward from Cape Agulhas (South Coast and Little Karoo), where the lower annual precipitation ranges from between 200 and 400 mm throughout the year, though often with a summer maximum, and often in the form of thunderstorms (Mahlalela et al. 2019; Van Niekerk

& Joubert 2011). The climate of this zone is influenced by the movement of warm, moist air from the Indian Ocean, producing all-year rainfall (Du Plessis and Scholms 2017). This region's climatic pattern is largely due to the subcontinent's location relative to low-pressure systems (between 40° and 50°S) (Midgley et al. 2005). Seasonally, when the westerly waves shift northward, these low-pressure systems bring rainfall to the southwestern part of the country in the form of cold fronts (Louw 2007). Thus, rainfall in the Western Cape is typically caused by cold fronts and associated extratropical cyclones, or by rare westerly disturbances such as cut-off lows, which frequently cause extreme rainfall events in the spring and autumn (Midgley et al. 2005). The Western Cape region is also influenced by coastal low-pressure systems, which generate hot, dry 'berg' winds that blow from the interior and cause above-average warm conditions in the spring and late winter (Louw 2007). However, it is the large variability in this dry climate that induces severe droughts in Western Cape.

The dominant soil types comprise sedimentary rocks (of the Malmesbury Group), which provide rich soil for agriculture (*e.g.*, viticulture and fruit farming under irrigation and rain-fed wheat cultivation) (DEADP 2011). The major land cover types include fynbos, renosterveld and succulent Karoo ecosystems (Lechmere-Oertel 1998). In this study, we focus on the Western Cape region's four river catchments: the Breede (12,348 km^2), Berg (7,715 km^2), Gouritz (45,715 km^2) and Olifants (46,220 km^2) (Fig. 1a). Additionally, The Breede basin accommodates the Theewaterskloof Dam (TWT) that serves as a crucial water source for the Western Cape, particularly for Cape Town. As the largest dam within the Western Cape Water Supply System, it boasts a storage capacity of 480 million cubic meters. This accounts for approximately 41% of the water accessible to Cape Town (Marais et al. 2021). The four Western Cape river catchments are rich in biodiversity and have high ecological importance but have been severely impacted by land-use change (DEADP 2011). For example, the Berg River is affected by urban effluent (near Cape Town) and high salinity while the Breede is affected by commercial forestation and alien invasive vegetation (Le Maitre et al. 2000).

2.2 Data

Several types of datasets were used to set up the model for this study. The datasets include observational data, reanalysis data, and model simulation data. We used QGIS 3.4 (Madeira) with QSWAT + plugin (version 1.2.2) to perform pre-processing of the SWAT + model input. We obtained global Digital Elevation Model (DEM) data from the Shuttle Radar Topography Mission (SRTM; CGIAR Consortium for Spatial Information; Jarvis et al. 2008) with a 90 m × 90 m resolution, digital soil data from the Food and Agriculture Organization's (FAO 2004; UNESCO available from Waterbase.Org) global soil databases (version 3.6), and digital land-use and land cover maps from the USGS Global Land Cover Characterization (GLCC; United States Geological Survey National Centre for Earth Resources; available from the Waterbase.Org) database (Table 1). Both observational and climate model simulation datasets were also analysed for this study. The observational data for this study includes the Global Meteorological Forcing Dataset (GMFD; version 3.0; Sheffield et al. 2006) that has been developed by Princeton University to drive models of land surface hydrology. The GMFD dataset is constructed by combining a suite of global observation-based datasets and it provides near-surface meteorological data. The dataset provides high resolution (0.5 degree) daily climate data that is available globally for 1901–2012. Climate model simulation data from the RCMs in the Coordinated Regional Climate Downscaling Experiment (CORDEX-Africa database website; Giorgi et al. 2009) were used (Nikulin et al. 2018). This consists of RCM data at a grid spacing of 0.44° X 0.44° (approximately 50 km) over the African continent. We used seven downscaled CMIP5 (Coupled Model Intercomparison Project Phase 5; Taylor et al. 2012) GCMs simulations for past and future climates (Table 2). Furthermore, to minimize the bias in

Table 1 Main SWAT + input data

Input Data	Source	Description	Reference
Digital Elevation Model (DEM)	Shuttle Radar Topography Mission; CGIAR Consortium for Spatial Information	90 m × 90 m resolution	Jarvis et al. 2008
Weather	Global Meteorological Forcing Dataset	0.5-degree, daily temperature, precipitation, relative humidity, solar radiation, wind	Sheffield et al. 2006
Stream network	Water Resources 2012	Stream network burn in (shapefile)	Herold & Bailey 2016
Land Use / vegetation cover	USGS Global Land Cover Characterization (v3.6)	Digital land-use and land cover maps (shapefile)	Waterbase.Org
Soil	Food and Agriculture Organization	Digital soil data (shapefile)	Waterbase.Org

Table 2 The CMIP5 GCMs simulations used in the study and the corresponding 30-year period for various global warming levels (1.5 °C, 2 °C, 2.5 °C and 3.0 °C) under RCP8.5 scenario. All the GCM simulations were downscaled with the RCA4 model in the CORDEX and bias corrected with MBCn in this study. Adapted from Déqué et al. 2017 in Naik and Abiodun 2020 (also see Appendix Table A1)

GCMs	Period of global warming levels (GWLs)			
	1.5 °C	2 °C	2.5 °C	3 °C
CanESM2	1999 – 2028	2012 – 2041	2024—2053	2034—2063
CNRM-CM5	2015 – 2044	2029 – 2058	2041—2070	2052—2081
CSIRO-Mk3-6–0	2018 – 2047	2030 – 2059	2040—2069	2050—2079
IPSL-CM5A-MR	2002—2031	2016 – 2045	2027—2056	2036—2065
MIROC5	2019—2048	2034 – 2063	2047—2076	2058—2087
MPI-ESM-LR	2004—2033	2021 – 2050	2034—2063	2046—2075
NorESM1-M	2019 – 2048	2034 – 206	2047—2076	2059—2088

the CORDEX dataset, we applied multivariate bias correction (N-dimensional probability density function transform; hereafter, MBCn) on the dataset using the method proposed by Cannon et al. (2015, 2018).

2.2.1 Characterizing droughts

Meteorological drought is typically defined by the amount of dryness (in comparison to some "normal" or average amount) and the length of the dry period (months or years) (NDMC 2021). Hydrological drought is associated with the effects of periods of precipitation deficits on surface and subsurface waters (i.e., streamflow, reservoir and lake levels, and groundwater) (Wilhite 2005). For this study, meteorological drought is characterized using Standardized Precipitation Index (McKee et al. 1993) and Standardized Precipitation Evapotranspiration Index (SPEI; Vicente-Serrano et al. 2010). Both SPI and SPEI are multiscalar meteorological drought indices, meaning they can provide drought information at various timescales. This versatility makes them suitable for detecting different types of droughts. Further details on the equation formulation and calculation for the drought index can be found in previous studies (e.g., McKee et al. 1993; Vicente-Serrano et al. 2010). Unlike SPI, SPEI can help identify droughts caused by a decrease in rainfall, higher atmospheric water demand (i.e., potential evaporation), or both. In addition, four types of hydrological drought were identified using soil water index (SWI), percolation index (PERCI), runoff index (RFI) and water yield index (WYLDI) indices over the Western Cape river basins. All the hydrological indices were calculated following a similar procedure as for SPI, but rainfall data were substituted with the relevant hydrological variable (see *e.g.,* Dutra et al. 2008; Sheffield et al. 2004; Shukla and Wood 2008). Input data for hydrological drought computation were derived from the SWAT + model. SWAT + calculates WYLD as the sum of surface runoff, lateral flow, and groundwater contributions, less transmission losses. Only the WYLDI for Theewaterskloof dam (TWT) is analysed in the study.

2.3 *SWAT+*

2.3.1 *SWAT + description and model set-up*

We used the Soil and Water Assessment Tool Plus (SWAT +). Compared to SWAT, SWAT + offers more flexibility, better independent modules (modularization), is more computationally efficient, and may result in enhanced model performance (Bieger, et al. 2017). SWAT is a spatially distributed, process-based hydrological model (Arnold et al. 2012). It is a small watershed to river basin-scale model and has been applied to a wide variety of watershed applications (see Akoko et al. 2021). As a time-continuous model with multiple components (including, for example, hydrology, soil, plant growth, nutrient transport, land management), it is designed to simulate the quality and quantity of surface and groundwater, and to predict the environmental impact of land-use, land management practices, and climate change. The SWAT model simulates watershed processes at the sub-basin scale, which is then further divided into Hydrological Response Units (HRUs). These are discrete areas of the same land-use, slope, and soil characteristics within the sub-basin.

The SWAT + was set up following the procedure described by Dile et al. (2016). We used the QGIS interface with the QSWAT plugin and default SQLite database (for data management), to delineate the basins, create HRUs and edit the climate inputs before running the model. QSWAT uses TauDEM (Terrain analysis using Digital Elevation Models) for watershed delineation. TauDEM provides a suite of geoprocessing capabilities (e.g., such as pit depression removal using the flooding approach, calculation of flow paths and slopes, calculation of contributing areas using single and multiple flow direction methods, delineation of stream networks using contributing area threshold, delineation of watersheds and subbasins; see Tarboton 1997). The standard specification library of Message Passing Interface (MPI; Gropp et al. 1996) was used to reduce the processing times of the DEMs. QSWAT was run with MPI installed and 20 processors selected. The delineation of the basins was generated using a burn-in vector file for a predefined stream network to accurately identify stream positions, and default threshold values (or number of DEM cells). The four primary catchments in the Western Cape were divided into 26 sub-basins and 234 landscape units (LSUs) and 2731 HRUs (Fig. 1d). Point sources were automatically added to each sub-catchment. The sub-basins were delineated with a 299 km^2 channel and 299 km^2 stream threshold. No merging of sub-basins was applied. We inserted a slope band of 10%, and no filtering was used in generating the HRUs. After the HRU generation, the SWAT + model assimilated the climate input (*i.e*., precipitation, air temperature, relative humidity, wind speed, and solar radiation) and used the Penman–Monteith approach to calculate potential evapotranspiration (PET). A map of land-use characteristics (Fig. 1b) shows that the region is dominated by cropland/grassland mosaic (CRGR, 30.74%), shrubland (SHRB, 27.89%), and grassland (GRSL, 23.13%). The remaining area is comprised of dryland cropland and pasture (CDRY; 9.02%), barren or sparsely vegetated (BSVG, 4.95%), savanna (SAVA, 1.69%), cropland/woodland mosaic (CRWO, 1.03%), evergreen broadleaf forest (FOEB, 0.69%), evergreen deciduous forest (FODB, 0.31%), mixed forest (FOMI, 0.43%), urban (URMD; 0.09%), or water (WATR; 0.02%). Soils in the Western Cape region are variants of loam and sandy loam (Fig. 1e). Loam predominates in the northern and eastern catchments (Olifants and Gouritz), whereas sandy loam is the prevailing soil type in the southern and western regions (Berg and Breede).

2.3.2 *SWAT + calibration and validation*

Model calibration is the process of estimating model parameter values to enable a hydrologic model to match observations. Model validation, however, is the process of demonstrating that a given site-specific model can make sufficiently accurate simulations (Arnold et al. 2012; Refsgaard 1997). For this study, daily streamflow data from 1 January 1980 to 31 December 1990 (11-year period) were used for calibration, and the remaining data from 1 January 1991 to 31 December 2005 (16-year period) were used to validate the model performance. For each catchment, the calibration and validation of the model were conducted over four hydrological stations across the region (E2H003, G1H013, H7H006 and J1H019; Fig. 1d; Herold, and Bailey 2016). The stations were chosen by considering the data quality and quantity for the calibration and validation periods. Validation ensures that the set of calibrated parameters performs reasonably well under an independent data set, *i.e*., without any further adjustment at different spatial and temporal scales (Neitsch et al. 2002). The calibration years were chosen because of the completeness of their observed data record and the inclusion of representative stations across the Western Cape's four primary river catchments (Berg, Breede, Olifants and Gouritz). The model parameters were selected for the calibration using the ± 30% change (from the default values) for 300 model simulations (after Yen et al. 2019). We examined the performance of the SWAT + model by comparison with observed data. Both graphical model evaluation techniques and statistical measures were applied. The statistical metrics used in the evaluations include the Nash–Sutcliffe model efficiency coefficient (NSE), percentage bias (PBIAS), root mean square error (RMSE), and coefficient of determination (R^2). The monthly calibration and validation of the SWAT + model for streamflow was performed using an automated Fortran program, following the Integrated Parameter Estimation and Uncertainty Analysis Tool + framework + (IPEAT + ; Yen et al. 2019). In this study ten model parameters (CN2, ESCO, EPCO, AWC, K, SURLAG, DELAY, REVAP_CO, REVAP_MIN; Table 3) were selected for the calibration using Nash–Sutcliffe model

Table 3 Selected model parameters for the SWAT + calibration and their associated best values based on Integrate Parameter Estimation and Uncertainty Analysis Tool framework (IPEAT + ; Yen et al. 2019) optimization using a range of ± 30% change in the default values

Parameter	Description	Unit	Object type	Best value (% change in the default value)
CN2	SCS runoff curve number	unit	HRU	-6.2
ESCO	Soil evaporation compensation factor	unit	HRU	-1.9
EPCO	Plant evaporation compensation factor	unit	HRU	-7.4
SOL_AWC	Soil available water storage capacity	mm_H20/mm	SOL	8.2
SOL_K	Saturated hydraulic conductivity	mm/hr	SOL	12.4
GW_DELAY	Groundwater delay, time required for water leaving bottom of the root zone to reach the shallow aquifer	days	GW	1.6
FLO_MIN	Water table depth for return flow	mm	GW	-12.9
REVAP_CO	Groundwater "revap" coefficient	unit	GW	12.4
REVAP_MIN	Threshold water depth in shallow aquifer for return to reach to occur	mm	GW	0.7
SURLAG	Surface lag coefficient, controls fraction of water entering reach in one day	days	BSN	7.6

Efficiency coefficient (*i.e.,* 1-NSE; hereafter NSE) as the objective function.

2.4 Climate change projection experiments

We applied the SWAT + model to perform climate change simulations for seven CORDEX experiments. These simulations are driven by the Representative Concentration Pathway (RCP) 8.5 scenario, which is the most realistic scenario of greenhouse gas emissions (Riahi et al. 2011). Here, the greenhouse gas emissions in the simulation's scenario increase considerably over time, leading to a radiative forcing of 8.5 W m^{-2} at the end of the century. The high-emissions scenario is frequently referred to as "business as usual" and represents a likely outcome if society does not make concerted efforts to reduce greenhouse gas emissions. Further information about the simulations can be found in Table 1 (see Appendix; Table A1). We assessed the impacts of climate change at various GWLs (*i.e.,* 1.5 °C, 2.0 °C, 2.5 °C, and 3.0 °C), and calculated the difference between the climate data in the reference period (1971–2000) and the GWL periods (*i.e.,* GWL minus reference).

2.5 Land-cover change experiments

SWAT + was applied to perform five experiments (Table 4). The first experiment (CTRL) represents the control scenario, *i.e.*, using the SWAT + default land-use pattern (Fig. 1b). The SWAT + land-use file was then modified to perform four additional experiments (Fig. 2a-d). The second experiment (FOMI) represents a future land-use scenario with an increase in invasive alien vegetation. Hence, mixed forest (represents alien invasive tree species; abbreviated FOMI) "invades" catchment areas outside their current distributional range. The main species that comprise these invasive species include eucalypts, pines, wattles, and particularly non-native species that have been identified as problematic to river catchments. These "alien" species often outcompete indigenous vegetation, disrupt ecosystems, and adversely impact biodiversity (Le Maitre et al. 2016; Kotzé et al. 2010). The area of land-use change for this scenario was delineated after consideration of the Working for Water programme that mapped the distribution of alien invasive tree species and identified invaded areas (riparian and non-riparian) across South Africa's quaternary catchments (Kotzé et al. 2010). The third experiment of land-use change (SHRB) describes a restoration of shrubland in areas covered by bare ground/sparse vegetation. The fourth scenario of vegetation change (CRDY) represents the expansion of crop (agricultural) practices to replace semi-natural vegetation (GRSL, CRGR and CRWO), while the fifth scenario describes a restoration of grassland to replace cropland areas (GRSL; Table 4). These experiments were not designed to simulate accurate scenarios of vegetation change, but rather to assess the magnitude and type of regional hydrological impact that might occur from a hypothetical, albeit potential, change in vegetation. Each change in LULC was implemented as a step-change to assess its impact. All the simulations were run for 148 years (1951–2099), but the simulation of the first five years was discarded as the spin-up period, and only the simulations of the remaining 143 years were analysed. The CTRL simulation was analysed to evaluate the performance of the hydrological model in simulating the Western Cape's climate, and to ascertain the projected future hydrological impacts that could be due to climate change and resulting changes in vegetation. All future projections of land cover change are provided as an anomaly (*i.e.*, those of FOMI, SHRB, CRDY and GRSL are relative to that of CTRL).

Table 4 Summary of land-use change experiments in the Western Cape river catchments

No	Experiments	Description of LULC pattern	Reference
1	CTRL	Control, SWAT + (default) land use	Figure 1b
2	FOMI	Increase in mixed forest (*i.e.*, eucalypt, pine, and black wattle trees invade river catchments) FOMI occupies 14.45% of the basin	Figure 2a
3	SHRB	Restoration of shrubland, shrubland replaces bare ground/sparsely vegetation areas SHRB replaces BSVG SHRB covers 32.74% of the basin	Figure 2b
4	CRDY	Expansion of (rainfed) agriculture cropland CRDY replaces GRAS, CRGR and CRWO CRDY covers 63.98% of the basin	Figure 2c
5	GRSL	Restoration of grassland, grassland replaces crop GRAS replaces CRDY, CRGR and CRWO GRAS occupies 63.98% of the basin	Figure 2d

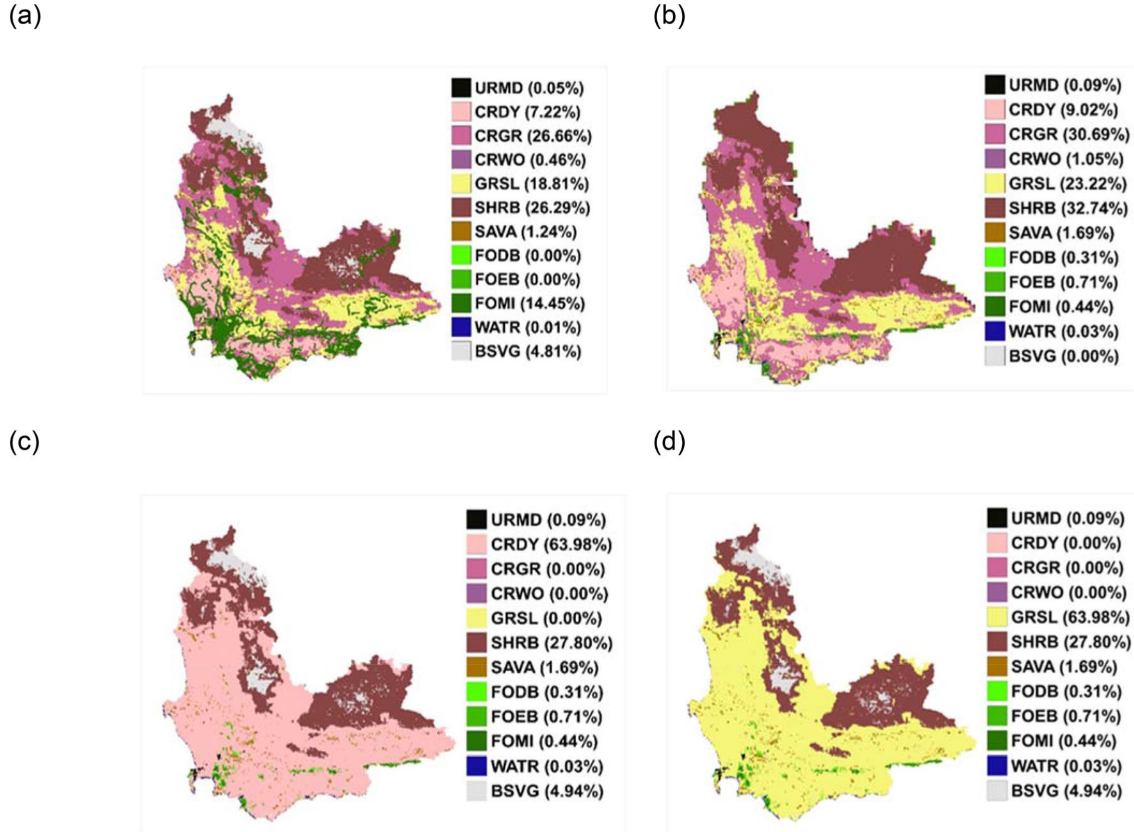

Fig. 2 The land use patterns used for each experiment: (**a**) FOMI, (**b**) SHRB (**c**) CRDY (**d**) GRSL. The land-use types are urban residential medium density (URMD), cropland/dryland and pasture (CRDY), cropland/grassland mosaic (CRGR), cropland/woodland mosaic (CRWO), grassland (GRSL), shrubland (SHRB), savanna (SAVA), forest—deciduous broadleaf (FODB), forest—evergreen broadleaf (FOEB), forest—mixed (FOMI), water (WATR), bare ground, sparsely vegetated (BSVG). Each land-use type (as a percentage across Western Cape) is indicated in brackets

3 Results and Discussion

3.1 *Evaluation of the hydrological model (SWAT+)*

There is a good agreement between the simulated and observed monthly streamflow at the four hydrological stations (*i.e.,* G1H013, H7H006, E2H003, and J1H019; Fig. 1d) during the calibration period (1980–1990) (Fig. 3). The simulated streamflow values closely track the observed values in reproducing seasonal and annual variations of the streamflow. The model also captures the observed peaks and their inter-annual variability. In the calibration period (1980–1990), the simulation spread often envelopes the observation, especially at H7H006 and E2H003. At two stations (*i.e.,* G1H013 and H7H006), the correlation between the simulated and observed flows is more than 0.5 and the NSE is also more than 0.5. The model also captures the differences in the magnitude of the streamflow across the stations. For instance, it agrees with the observation that, among the four stations, the streamflow is largest at H7H006 (*i.e.,* Breede river) and G1H013 (*i.e.,* Berg river) and lowest at J1H019 (*i.e.,* Gouritz river). However, there are some notable model biases in the simulation. The model overestimates the magnitude of the peaks in some years and underestimates them in others. For instance, it overestimates the observed streamflow by more than 40 $m^3 s^{-1}$ at H7H006 in 1986 and underestimates it by up to 120 $m^3 s^{-1}$ at H7H006 in 1983. The model percentage bias (PBIAS) ranges from -43% (at G1H013) to 73% (at J1H09). Several reasons can be attributed to the model biases, ranging from shortcomings in model development to uncertainties in model input and set-up. For example, the underestimation of the streamflow conditions may be due to overestimation of evaporation. Unfortunately, there is no evaporation data for further analysis on the biases. The biases may also be due to errors that exist within the climate and hydrological datasets. The resolution of the GMFD reanalysis may be insufficient to fully resolve all the climate processes in the Western Cape's complex topography. The resolution of the soil and land-use dataset may also be too coarse to represent all the hydrological processes in the catchments. This problem has also been reported and identified in previous studies that applied

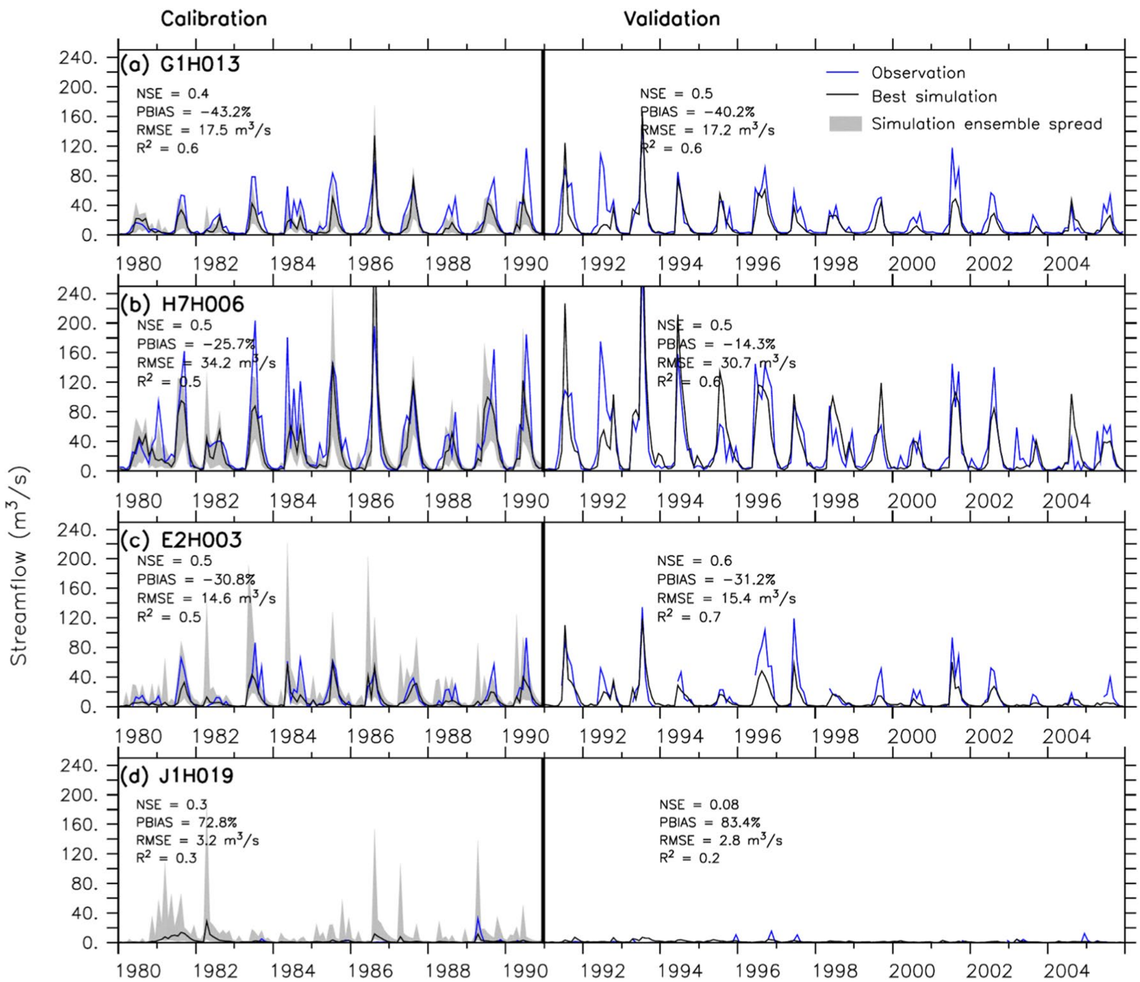

Fig. 3 Comparison of the observation and SWAT + simulated streamflow during the calibration and evaluation periods at four hydrological stations (*i.e.,* G1H013, H7H006, E2H003 and J1H019) in the Western Cape river catchments. The values of the statistical metrics (*i.e.,* NSE, PBIAS, RMSE, and R^2) used in quantifying the comparison are indicated

SWAT over South African catchments (*e.g.,* Dabrowski 2014). The biases may also occur from using naturalised flow data as observed streamflow, since this removes the effects of human impacts (*e.g.,* reservoirs, dams) to estimate the unimpaired flow hydrology.

Nevertheless, the model's performance in this catchment is deemed satisfactory. In most cases, the model performance is better (or the same) during the validation period (1991–2005) than in the calibration period (1980–1990) (Fig. 3). For instance, at station G1H013, the model performance improves for NSE (from -0.4 to 0.5), PBIAS (-43.2% to -40.2%), and RMSE (from 17.5 $m^3 s^{-1}$ to 17.2 $m^3 s^{-1}$). Also, at station E2H006, it improves for PBIAS (from -25% to -14%), RMSE (34.2 $m^3 s^{-1}$ to 30.7 $m^3 s^{-1}$), and for R^2 (from 0.5 to 0.6). However, the model improvement depends on statistical metrics used in the performance evaluation. For example, at station H7H003, while the model performance improves for NSE (from 0.5 to 0.6) and R^2 (0.5 to 0.7), it deteriorates for PBIAS (-30.8% to -31.2%) and RMSE (14.6 $m^3 s^{-1}$ to 15.4 $m^3 s^{-1}$). The difference in model performance in the two periods may be due to differences in dominant processes or differences in the lengths of the observation data gaps in the periods, as evident in station J1H019, where the paucity of observation data makes the results unreliable. In accordance with established model evaluation criteria outlined by Moriasi et al. (2007; 2015), the NSE exceeds 0.50, and the PBIAS remains within + 25% for streamflow, particularly notable for Stations H7H006 and E2H003. Results obtained from the evaluation of the SWAT model in this study are consistent with findings from previous studies conducted over other river basins in South Africa. These studies show good transferability of the SWAT for understanding hydrological processes as show good agreement between the simulated and observed streamflow with satisfactory model performance. Andersson et al. (2011) showed the value of model calibration reduced the predictive uncertainty of the model over the Thukela River Basin. Welderufael et al. (2013) also showed good performance of SWAT in simulating the monthly streamflow over the Modder River Basin (NSE of 0.57 for the calibration). Gyamfi et al. (2016b) found satisfactory model performance in both the calibration and validation periods (i.e., NSE and R^2 values were greater than 0.6, and PBIAS values in the range of $\pm 10\%$), but in contrast to our findings however, SWAT performed better (or the same) during calibration period than in the validation period. Nevertheless, the generally good performance of the SWAT + model at the stations suggests that the model provides a reliable representation of hydrological processes in Western Cape catchments, as is needed in this study.

3.2 Evaluation of the climate simulation datasets (CORDEX)

To provide confidence on the quality of the climate simulation datasets (CORDEX), which are used as input data in the SWAT + hydrological projections, we examine the performance of the CORDEX simulations (with and without bias-correction) during the historical period (1971–2000). In the evaluation, we compare the performance of the original CORDEX dataset (CORDEX_ORG) with the multivariate bias corrected CORDEX dataset (CORDEX_MBCn). With reference to the reanalysis data (GMFD) results, the model evaluation focuses on how well the dataset reproduces different climate variables (*e.g.,* mean temperature (Tmean), precipitation (PRE), potential evaporation (PET) and evaporation (ET)), and how accurately SWAT + replicates the

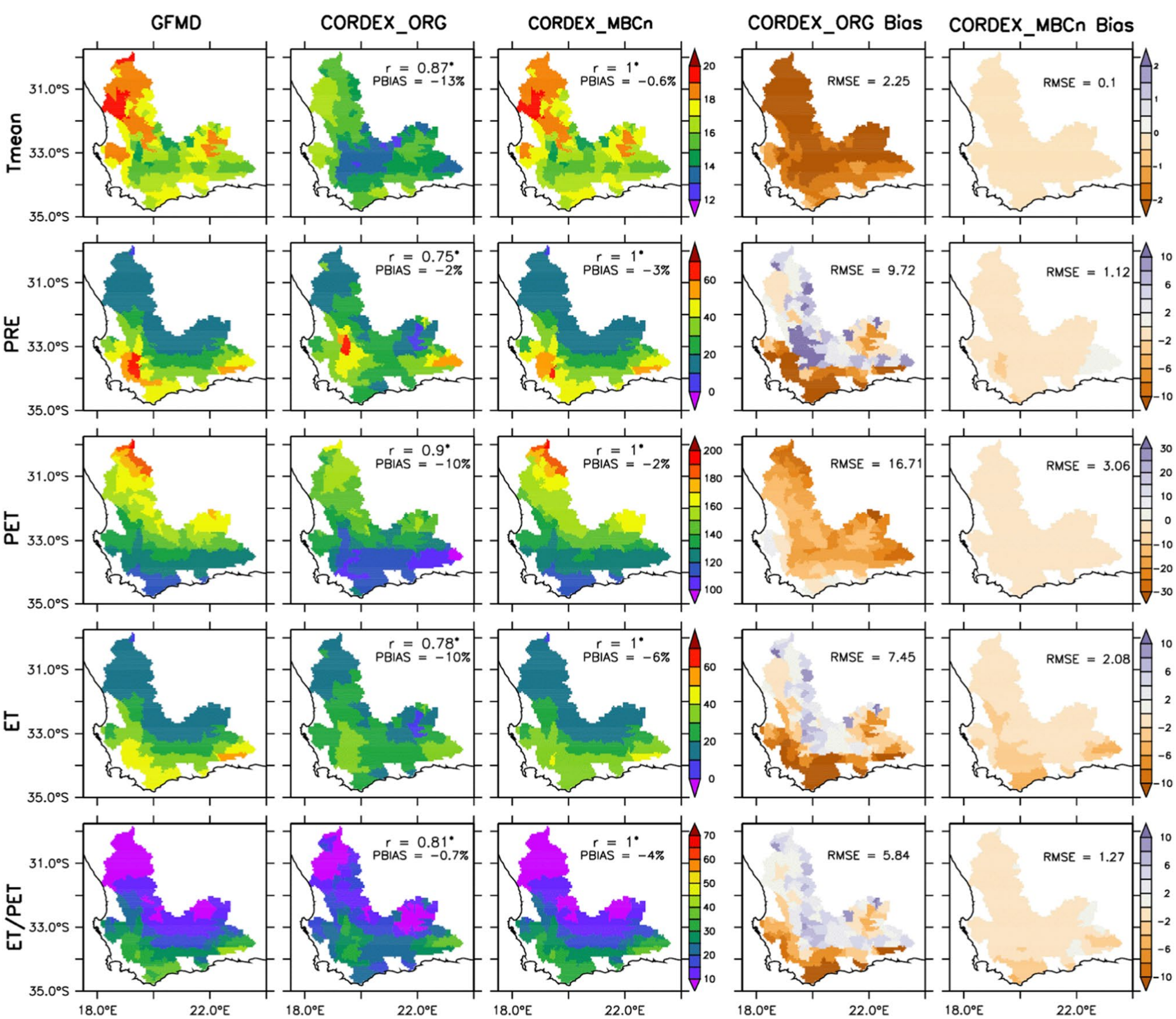

Fig. 4 Spatial distribution of climate variables over the Western Cape river catchments as simulated by SWAT + using GMFD

hydrological variables (*e.g.,* soil water (SW), percolation, runoff, streamflow, and stream ET) over the catchments.

The CORDEX_ORG simulation captures the spatial distribution of climate variables across the Western Cape, but with some notable biases (Fig. 4). The MBCn bias correction reduces the errors (PBIAS) and improves the correlation (r) between the CORDEX and GMFD results. For example, the bias correction reduces Tmean PBIAS from -13% to -0.6% and increases the r from 0.87 to 1.0. Although it does not improve on PRE PBIAS, it increases the r from 0.75 to 1.0. However, the corrected dataset (*i.e.,* CORDEX_MBCn) generally improves on the original dataset (CORDEX_ORG) and reproduces the spatial distribution of climate variables better. In agreement with GMFD, CORDEX_MBCn simulates the highest temperature over the north-western part of the basin and the lowest temperature over the mountain range at the centre of the study domain. It also captures the location of the maximum PRE on the south-western side of the mountain. Both datasets (GMFD and CORDEX_MBCn) agree on the difference in spatial distribution of PET and ET over the region. While PET increases from south to north, ET increases from north to south, suggesting the spatial distribution of evaporation of the basin is more driven by water availability (PRE) rather than by atmospheric demand (PET). However, in both datasets, the capability of the Western Cape catchments in meeting the atmospheric demand (*i.e.,* ET/PET) decreases from south-west to north-east in accordance with PRE distribution. Generally, the capability of catchments to meet the atmospheric water demand is

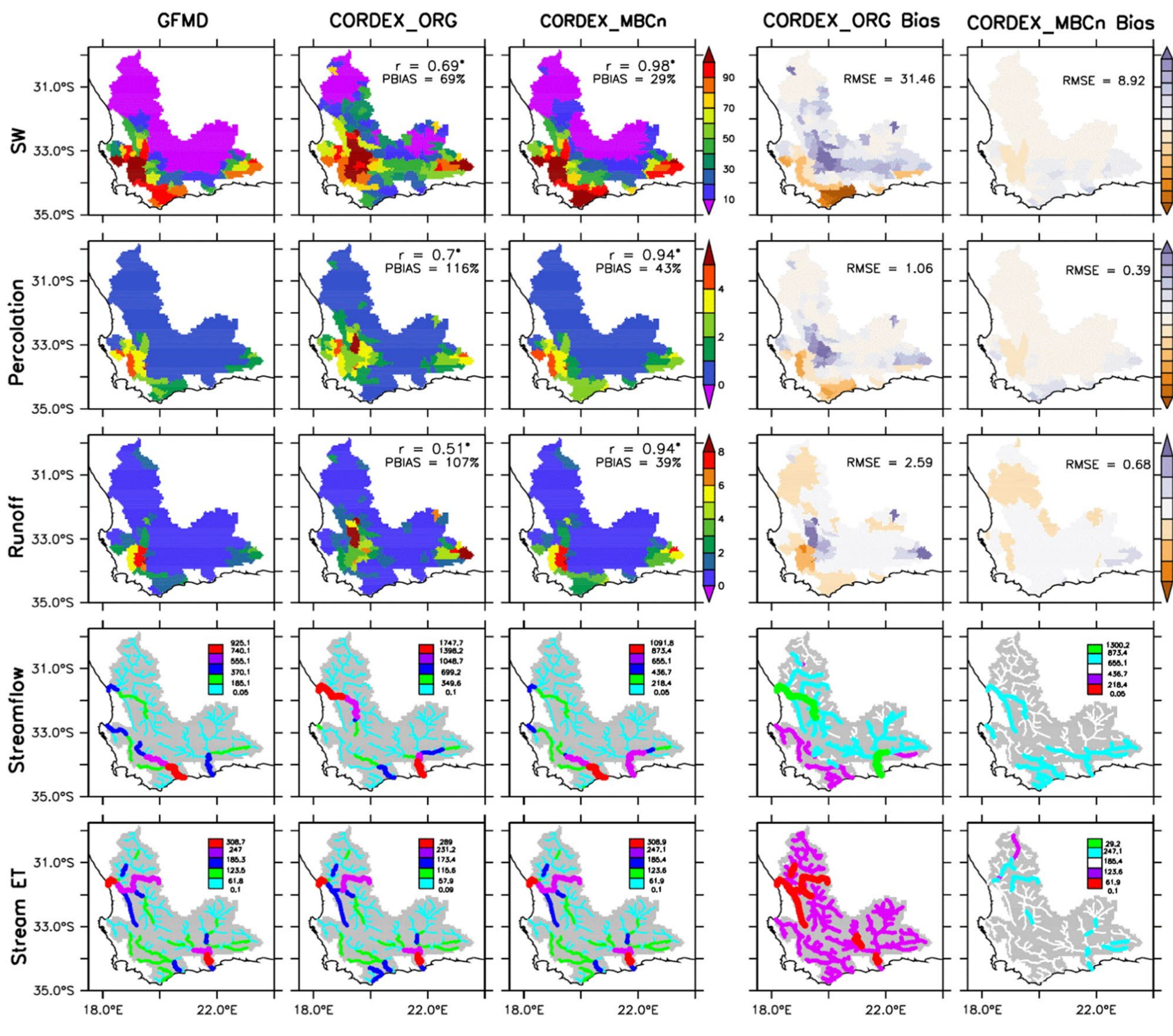

Fig. 5 Same as Fig. 4 but for hydroclimate variables

higher over the Berg and Breede than over the Olifants and Gouritz.

The bias correction of the CORDEX dataset also improves the hydrological simulations over the catchments, but the performance of CORDEX_MBCn is lower for hydrological variables (i.e., 29% ≤ PBIAS ≤ 116%) than for climate variables (-6% ≤ PBIAS ≤ -0.6%) (Fig. 5). However, in reference to GMFD results, the CORDEX_MBCn still captures the spatial distribution of hydrological variables across Western Cape well. For instance, in both datasets, the spatial distributions of SW, percolation, and runoff follow that of PRE. In contrast to CORDEX_ORG, CORDEX_MBCn agrees with GFMD that the Breede catchment features the highest streamflow, while the Gouritz river has the lowest. Nevertheless, in both datasets, the ET is higher over the Gouritz than over the Breede. This is because PET is higher over the former than the latter, and as long as there is water in a river, the ET over the river is not limited by a lack of precipitation or by low soil moisture.

3.3 Impacts of climate change on climate and hydrological variables

Figure 6 shows the timeseries of projected climate changes across the Western Cape for the period 1980–2100. These projections show a gradual increase in mean temperature (Tmean), from about 1 °C in 2030, and reaching about + 4 °C by the end of the century. The spatial distribution of the warming is generally uniform across the region, but the magnitude of the warming increases with the GWLs (Fig. 7). For example, the temperature increase is projected to be between 1.5 – 2.5 °C under GWL1.5 and GWL2.0, or as high as 3.0 – 4.5 °C under GWL2.5 and GWL3.0 across the catchments. These climate projections for temperature are in line with those of previous studies,

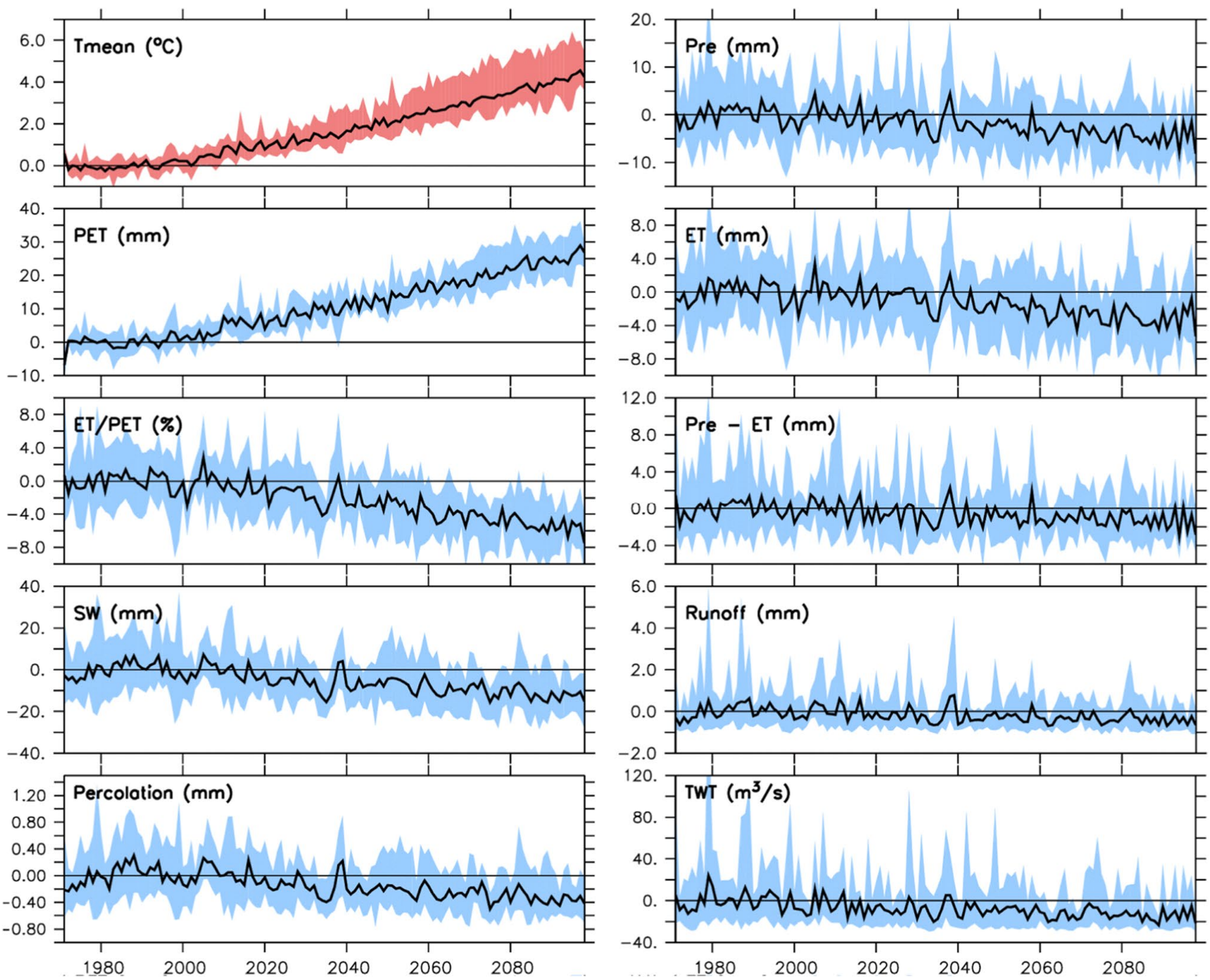

Fig. 6 Time series of hydroclimate variables over the Western Cape (1971—2099)

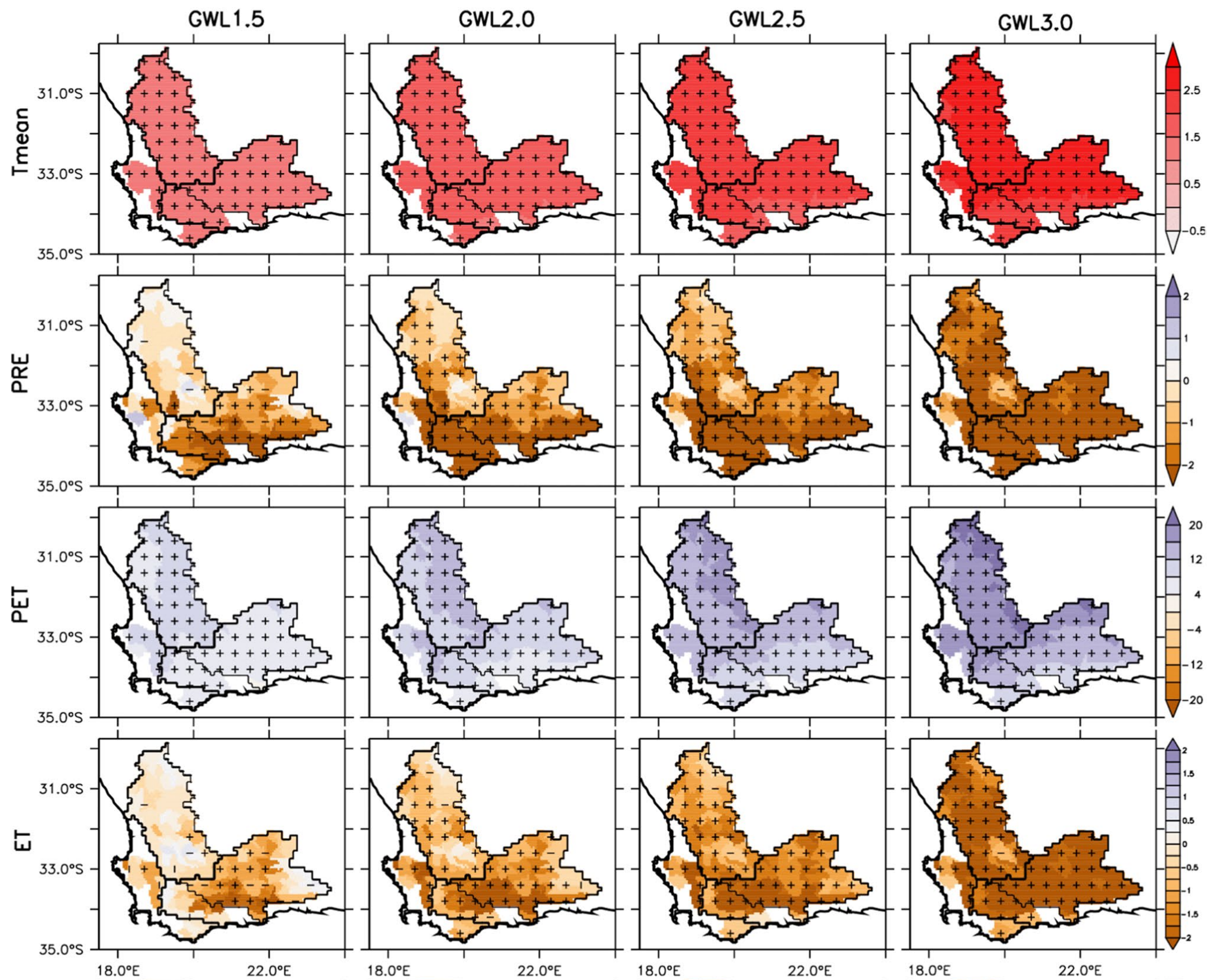

Fig. 7 Spatial distribution of projected changes in climate variables over the Western Cape catchments at four global warming levels (GWL1.5, GWL2.0, GWL2.5, and GWL3.0). The vertical strip (|) indicates where at least 80% of the simulations agree on the sign of the changes, while horizontal strip (−) indicates where at least 80% of the simulations agree that the projected change is statistically significant (at 99% confidence level). The cross (+) shows where both conditions are satisfied; that is, the change is robust

which suggests increased temperatures (up to 4 °C) could occur in this region before the end of the century (Haensler et al. 2011; Field et al., 2014; Naik and Abiodun 2016). Note that for higher GWLs, increased warming tends to occur further inland, over the north-eastern regions. For example, under GWL3.0, the increase is about 4.5 °C, over the north-eastern parts of the Olifants catchment, but about 2.5 °C along southern parts of the Berg and Breede. This is in line with previous projections and may be due to the moderating effects of the ocean on temperature along the coastline (*e.g.,* Mbokodo et al. 2020; Naik and Abiodun 2020). This projected increase in temperature leads to an increase in potential evaporation (PET), which also shows a gradual increase by the end of the century (from about + 10 mm mon^{-1} in 2030, and to about + 20 mm mon^{-1} by 2100; Fig. 6). The areas where the largest changes in PET occur compare well spatially to areas where the largest changes in Tmean occur (Fig. 7), and the magnitude of the PET change increases with higher GWLs (2.0, 2.5 and 3.0). The largest increase occurs over north-eastern parts of the Olifants and northern Gouritz catchments, where PET is projected to increase by + 10 mm mon^{-1} (GWL1.5) to more than + 20 mm mon^{-1} (GWL3.0), respectively. Several studies confirm that PET rates may increase with higher temperatures in the future. This is because global warming (and associated higher temperatures) lead to an increase in the vapor pressure deficit of air and increased atmospheric evaporative demand (Dai et al. 2018; Yuan and Bai 2018).

The projected changes in precipitation (PRE) are more complex than those of Tmean. PRE projections show no discernible change in the trend before 2040, but a decreasing trend afterwards until the end of the century. Nonetheless, the pattern of the PRE change differs spatially across the Western Cape catchments. While there is a general decrease in PRE across the region, the projections under GWL 1.5 suggest more drying (about -2 mm month^{-1}) may occur over some areas, like parts of the southern Gouritz and the south-eastern Breede, while only modest change occurs over other areas, like the central Olifants. Generally, this pattern is similar across the GWLs, only that the magnitude of the change increases under higher GWLs and that the spatial extent of the drying increases. For instance, the area of maximum drying includes the southern margin of the Gouritz and Berg (-1.5 mm mon^{-1}) for GLW2.0, and it extends cross the entire Gouritz, Breede, and parts of the Berg and Olifants, where it exceeds -2.5 mm month^{-1} for GWL 3.0. Only a few areas show wetter conditions over the Western Cape in the future. The exception to the general drying over the region occurs over a limited area of the central Berg (near the large dams), where increased PRE (+ 2 mm mon^{-1}) occurs, and over central-southern parts of the Olifants (+ 1 mm mon^{-1}). However, this occurs for GWL1.5, but not under higher GWLs, when the drying signal dominates. The large-scale forcing mechanisms potentially responsible for the decreased rainfall across the Western Cape region may include an increase in the intensity and frequency of upper-level highs, and migration of subtropical anticyclones towards the mid-latitudes across the Southern African subcontinent (Sousa et al. 2018). This poleward shift of the Southern Hemisphere moisture corridor and the displacement of the South Atlantic storm-track may create significantly drier conditions under conditions of future climate change. The projected evaporation (ET) can be linked to the changes in PRE. While there is no discernible trend in future ET timeseries projections over the Western Cape (Fig. 6), there are changes spatially over the Western Cape. The spatial pattern of the ET change is not uniform across the Western Cape for GWL1.5. ET may decrease over catchments, such as the Gouritz (-2 mm mon^{-1}), but increase over others, such as the south-central Olifants (+ 1 mm mon^{-1}) or the Berg (+ 1 mm mon^{-1}). Generally, however, the areas where the largest changes in ET occur are comparable to the areas where PRE changes occur. The magnitude of the ET change also increases with higher GWLs (2.0, 2.5 and 3.0). For example, the projections show that, for higher GWLs, ET may decrease over much of the region (-1.5 mm mon^{-1}), and particularly over the south-western Gouritz and central Olifants. This decrease may be up to -1.5 mm mon^{-1} under GWL1.5, -2 mm mon^{-1} under GWL2.0 and exceed -2.5 mm mon^{-1} under GWL3.0.

The projected decrease in hydrological variables can be linked to the decrease in PRE (Figs. 6 and 7). The spatial distribution of these hydrological changes is consistent with that of PRE. For example, the projections show a general decrease in soil water (SW) across the region (-10 mm mon^{-1}), that is enhanced over the eastern Olifants (-20 mm mon^{-1}) and the central Berg (-20 mm mon^{-1}), under GWL3.0. The spatial distribution of the drying is comparable for higher GWLs, except that the magnitude of the drying increases with the GWLs. This is because the projected decrease in PRE negatively affects the overall soil water budget of the affected areas. With time, this causes a gradual decrease in volumetric water content of soil over the region (SW; about -10 mm) from 2050–2100 (Fig. 6). This negative change in storage (*i.e.,* SW content) occurs when outputs, such as percolation (PERC) and surface runoff (RUNOFF) exceed PRE. As seen in Fig. 7, the distribution of the future drying is spatially comparable for these variables. Since the soil does not reach saturation, reduced PERC occurs and there is also a consistent decrease in overland RUNOFF. (Note the differences in PERC and runoff are comparable to the spatial variation in soil types (Fig. 2e), because loam and sandy loam textures differ in their water-holding capacity.) This is consistent with our projected changes in hydrological variables over channels (Figs. 8 and 9). There is a decrease in channel precipitation over many stream areas of the Western Cape (Stream PRE; -10 mm mon^{-1}), and this drying increases under higher GWLs. For instance, drying of -8.4 mm mon^{-1} occurs along channels of the southern Gouritz and Breede, under GLW2.0, and it extends across the entire Western Cape, where it exceeds up to 16.9 mm mon^{-1} for GWL 3.0. The projected increase in PET leads to an increase in stream ET, which occurs for all GWLS, and over all the Western Cape catchments, but is enhanced over the Olifants and Gouritz catchments (+ 19 mm mon^{-1}). Since more water is lost through evaporation, there is an associated decrease in streamflow over many of the region's channels (+ 10 mm mon^{-1}), but particularly over the Olifants and Gouritz catchment (+ 19 mm mon^{-1}). This is consistent with the decreasing trend in future projection of channel discharge entering the largest dam in the Western Cape at Theewaterskloof (TWT; Fig. 6) and reaching about -2 m^3 s^{-1} by the end of the century. While there are few studies on the hydrological projections for the Western Cape, several studies recognize that this region has historically experienced increased surface aridity due to decreased precipitation. The hydrological projections here are in line with historical analysis, which found increased surface temperature, decreases in precipitation, and occurrence of dry spells, which have depleted water resources in the Southwest Cape (Jury 2018).

3.4 Impacts of land-use change on hydrological variables

The land-use changes have different impacts on the future hydrological water balance due to their influence on the curve number (CN; Fig. 10). With FOMI, there is a decrease

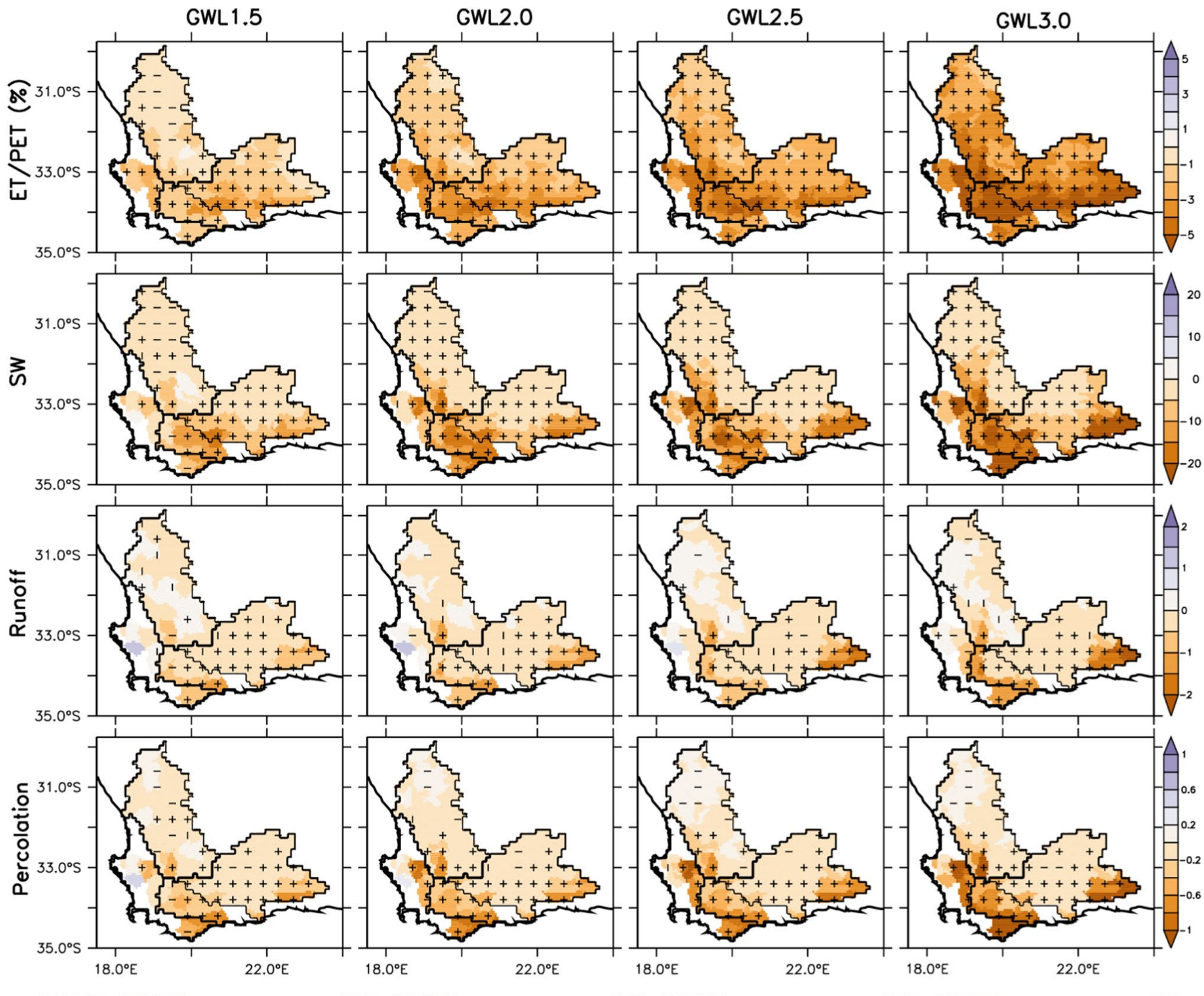

Fig. 8 Same as Fig. 8, except for hydrological variables

in CN, which is consistent with the area of mixed forest land-use change (CN of about -3, Figs. 10 and 2a). The lower runoff potential is linked to more permeable soil surface and hence, there is less runoff from rainfall. As such, FOMI increases the amount of soil water (SW) available over the catchment. For instance, SW increases occur over parts of the southern Berg (+2 mm mon^{-1}) catchment, and the southwest Breede (+2 mm mon^{-1}) catchment. The increase in SW may be due to the deeper rooting network of trees, which alters the physical properties of the upper soil layers, improving infiltration and percolation. As the amount of available SW at the surface increases, more water is available for conversion through evapotranspiration (ET). Thus, for FOMI, ET also increases over these parts of the Berg and Breede (+0.5 mm mon^{-1}) that are spatially comparable to that of SW. Although FOMI generally decreases runoff over the region (-0.2 mm mon^{-1}), particularly over parts of the central Berg and western Breede (-0.5 mm mon^{-1}), it also increases the streamflow over most catchments. The largest increases in streamflow occur over parts of the western Olifants, the northern Berg, and the south-eastern Gouritz (about +61.9 m^3 s^{-1}; Fig. 10). Decreases in streamflow occur only in some sub-basins of the western Breede and southern Berg (about -61.9 m^3 s^{-1}). These hydrological changes suggest that the increase in streamflow is unlikely due to surface runoff (from precipitation runoff over the landscape *i.e.,* overland flow) but rather due to percolation of water past the soil profile (subsurface) to become groundwater recharge, or via lateral movement in the profile (interflow), which eventually reaches streamflow (not shown). Several studies confirm that forests may have a positive impact on soil hydraulic properties, by functioning as water harvesters and contributing to infiltration, deeper

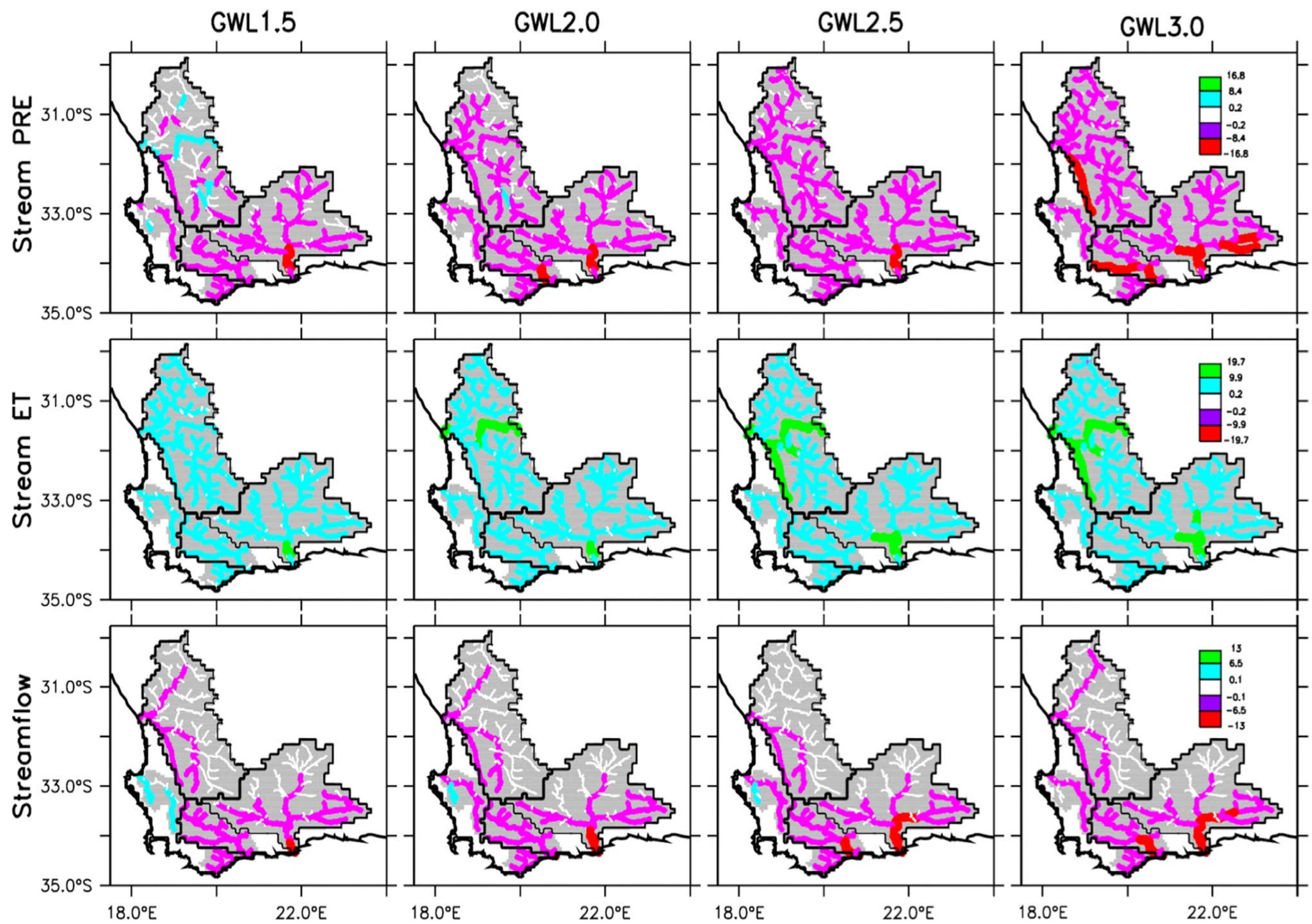

Fig. 9 Same as Fig. 8, except for river channel variables

drainage, and groundwater recharge (*e.g.,* Bargués Tobella et al. 2014; Luo et al. 2020).

The hydrological impact of SHRB is similar to that of FOMI. With SHRB, there is a decrease in CN (of about 8) over the areas where shrubland restoration replaces bare ground (Figs. 10 and 2b). This occurs particularly over sub-basins of the northern and central Olifants and northern Gouritz. Over the central and northern Olifants sub-basins, SHRB increases SW (+2.0 mm mon^{-1}) and increases ET (+0.4 mm mon^{-1}). But SHRB decreases runoff over the region (-0.2 mm mon^{-1}), particularly over the central Olifants and northern Gouritz (-0.5 mm mon^{-1}). However, unlike FOMI, SHRB decreases water yield over most Western Cape catchments. The streamflow decreases (about -61.9 m^3 s^{-1}) occur over the Olifants, Gouritz and Breede. However, SHRB does not influence water yield over the Berg since no land-use change occurred in this catchment. Overall, these hydrological changes suggest that the restoration of shrubland may decrease streamflow and may have negative impacts on the water security of the region. Nevertheless, it is crucial to acknowledge the limitations in extending these findings to implications for regional ecology conservation. Removing shrubland vegetation may lead to adverse impacts, as it eliminates the protective barrier and leaving bare ground exposed to erosion.

The response of CRDY is complex, as it includes both increases and decreases in hydrological conditions. CRDY (*i.e.,* expansion of cropland/dryland area) increases the curve number (CN), such that the area of LUC is spatially consistent with the area of higher CN (about + 5; Figs. 10 and 2c). While CRDY decreases SW over some sub-basins, it increases it in other sub-basins. For instance, it decreases SW over the eastern and southern Berg (-2 mm mon^{-1}), the northern and southern Breede (-2 mm mon^{-1}) and the eastern Gouritz (-1.6 mm mon^{-1}), but it increases SW over the southwestern Olifants (+0.8 mm mon^{-1}). However, the hydrological response of CRDY differs from FOMI, in that, while the SW changes are spatially consistent with ET in some catchments, they are not consistent in others. For instance, the decrease in ET (-2 mm mon^{-1}) over the Breede is consistent with the decrease in SW over the catchment, and the increase in ET (+0.4 mm mon^{-1}) over the southwestern Olifants also agrees with the increase in SW over this sub-basin. However, the increase in ET (+0.2 mm mon^{-1}) over

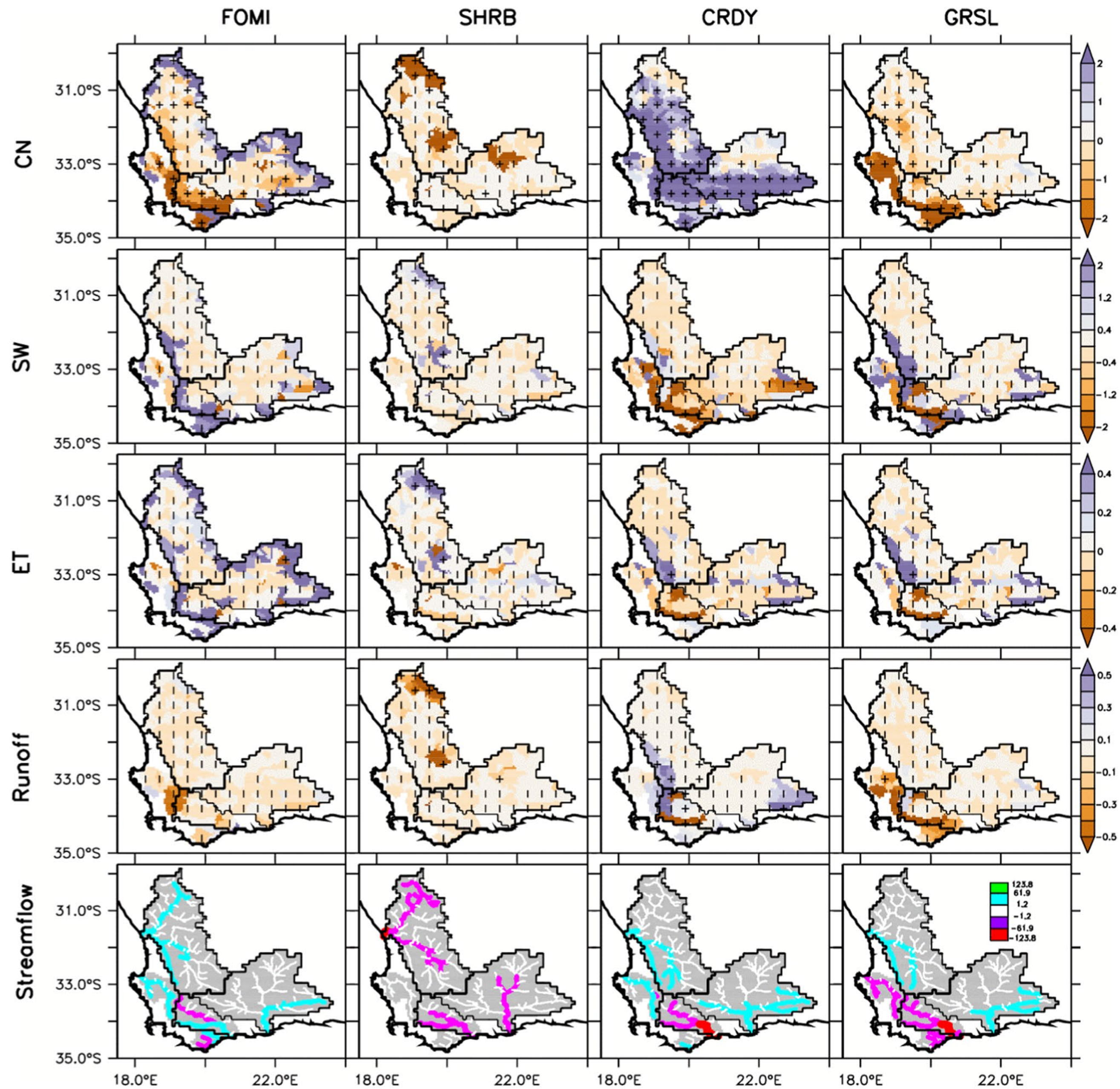

Fig. 10 Impact of land use changes on hydrological variables in the Western Cape catchments. The vertical strip (|) indicates where at least 80% of the simulations agree on the sign of the changes, while horizontal strip (−) indicates where at least 80% of the simulations agree that the projected change is statistically significant (at 99% confidence level). The cross (+) shows where both conditions are satisfied; that is, the change is robust

the southern Breede is not consistent with the decrease in SW over the sub-basins. Moreover, CRDY increases runoff and streamflow over the southern Olifants and eastern Gouritz (+ 0.5 mm mon^{-1} and about + 61.9 m^3 s^{-1}) but decreases them over much of the Breede (-0.5 mm mon^{-1} and up to about -123.8 m^3 s^{-1}, respectively). Unlike with FOMI, the increase in the streamflow obtained with CRDY is likely due to an increase in surface runoff over the landscape. It may be that the percolation rate is slower with CRDY than with FOMI. Nevertheless, the CRDY changes have complex impacts on the hydrology of the region, possibly due to the complex topography and local soil conditions.

The hydrological response to GRSL is also complex. GRSL (*i.e.*, restoration of grassland) generally decreases the curve number (CN), with areas of lowest CN spatially consistent with areas converted from CRDY to GRSL (CN about -4; Figs. 10 and 2d). GRSL is associated with a lower curve number (compared to CRDY) and hence, less runoff from rainfall. Compared to CRDY, GRSL increases SW over many catchments. For example, SW increases occur over the southwestern Olifants (+ 2 mm mon^{-1}), the eastern Gouritz (+ 2 mm mon^{-1}) and several sub-basins of the Berg. Although, like CRDY, for GRSL SW decreases occur over the southern margins of the Breede (-2 mm mon^{-1}). Even so, the changes in ET for the two land-uses (CRDY and GRSL) are spatially comparable. Nevertheless, unlike CRDY, GRSL reduces runoff (-0.5 mm mon^{-1}) over many subbasin areas of the four catchments. And, while changes in streamflow for the two land-uses are similar over the Olifants and Gouritz catchments (increases), and over the Breede (decreases), unlike CRDY, GRSL reduces streamflow over the Berg (-61.9 m^3 s^{-1}).

3.5 A comparison of the impacts of land-use change with climate change projections

The impacts of projected future climate change resulted in decreased hydrological variables over the catchments studied herein, but the percentage decrease varies (Fig. 11a). For instance, while the ET decreases by only 10%, the percolation (PERC) decreases by more than 40%. The decrease in ET may be linked to the projected decreases in PRE, which makes less water available for evaporation over the catchments. The capability of the basin to meet atmospheric water demand (ET/PET) also decreases (by -20%), not only because the ET decreases, but because PET, the atmospheric water demand, is also projected to increase across the catchments (Fig. 8). These changes drive the decrease in other hydrological variables because they alter the overall soil water budget of the catchment areas, inducing a 30% decrease in soil water (SW), a 40% decrease in percolation (PERC) and a 30% decrease in runoff. Water yield also decreases as less water percolates into deep soil layers. Hence, there is a decrease in water yield (-30%) and discharge (-40%) at the Theewaterskloof dam (TWT). The impacts of some land-use changes offset the climate change impacts on the mean hydrological variables (Fig. 11a). For example, CRDY could result in increased runoff by 10%. This could mitigate the impacts of climate change on runoff by about 30%. CRDY may also offer potential climate change offset due to its impact on water yield at the Theewaterskloof dam (TWT; + 5%), where CRDY may increase discharge. Flörke et al. (2018) also determined that, in the context of future climate change, enhancements in agricultural water usage could potentially release enough water to meet the needs of urban areas. Nevertheless, for FOMI, SHRB, and GRSL land-use changes, the impact on the hydrological variables is almost negligible relative to the impact of future climate change.

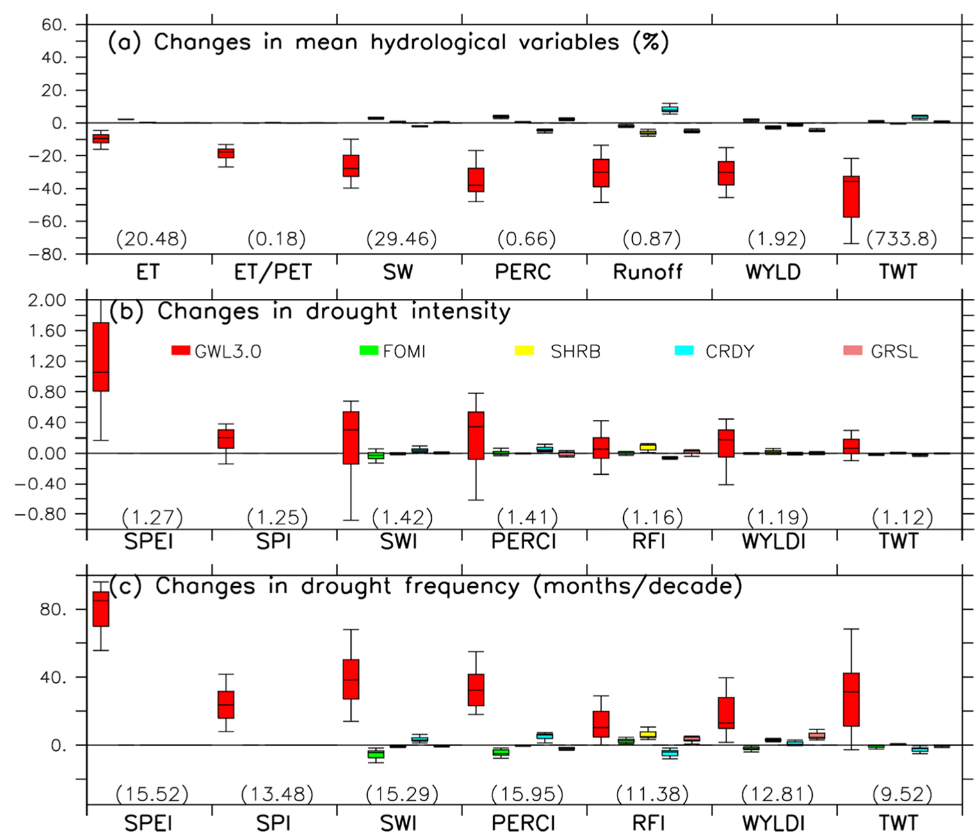

Fig. 11 A comparison of impact of land cover change and climate change projection on hydrological variables in Western Cape catchments

The changes in the hydrological variables are linked to changes in drought. The projections indicate that impacts of climate change could increase drought frequency in the future. Climate change may increase both Standardized Precipitation Evapotranspiration Index (SPEI) (about + 80 months decade^{-1}) and Standardized Precipitation Index (SPI) (+ 20 months decade^{-1}) drought frequency (Fig. 11c). Note that for both indices, a moderate drought is defined as a condition in which the drought index (SPI or SPEI) is less than or equal to − 1.0 (i.e., moderate drought). These projections are in line with those of a previous study, which suggests that changes in the intensity and frequency of droughts are weaker when using the SPI than the SPEI, and that SPI projections may in fact underestimate the influence of global warming on drought because they do not account for the influence of PET (Naik and Abiodun 2020). The changes in the SPEI/SPI drought provide the upper/lower range that is linked to changes in hydrological drought for other variables. For instance, climate change may increase the frequency of the soil water drought index (SWI) by + 38 months decade$^{−1}$, the percolation drought index (PERCI) by + 30 months decade$^{−1}$, the runoff drought index (RFI) by + 10 months decade$^{−1}$, and the water yield drought index (WYLDI) by + 12 months decade$^{−1}$. Some land-use changes may offset the climate change impacts on the hydrological drought variables (Fig. 11). Most notably, since FOMI may increase the soil water index (SWI) and the percolation index (PERCI), it may thus reduce the impacts of climate change on runoff drought by about -5 months decade$^{−1}$. Similarly, since CRDY may increase runoff (RFI), it also offers a climate change offset due to its impact on decreasing the frequency of runoff drought by about -5 months decade$^{−1}$. At the Theewaterskloof dam (TWT), CRDY may increase discharge, and partially offset the frequency of discharge drought by about -3 months decade$^{−1}$. For GRSL land-use changes, the impact of the hydrological variables on drought is almost negligible relative to the impact of future climate change drought or it may even enhance it (*e.g.,* for RFI).

4 Conclusion

In this study, the SWAT + was used to perform hydrological simulations over four Western Cape river catchments. We calibrated the SWAT + and evaluated its performance in reproducing the hydrological variables over the region. We then examined the MBCn bias correction method and its influence on the climate dataset, quantified the potential impacts of future climate change on drought across various global warming levels (GWLs 1.5, 2.0, 2.5, 3.0 °C), and examined the impact of four land-use changes on hydrological drought. We used the Standardized Precipitation Index (SPI) and the Standardized Precipitation Evapotranspiration Index (SPEI) to quantify drought frequency and intensity. The results of the study can be summarized as follows:

- Model evaluation shows good agreement between the simulated and observed monthly streamflows at the four hydrological stations (*i.e.,* G1H013, H7H006, E2H003, and J1H019) during the calibration period (1980–1990). The simulated streamflow also tracked the observed values in reproducing seasonal and annual variation of the streamflow, and the model captured the inter-annual variability. Generally, the model provided a satisfactory representation of hydrological processes in Western Cape river catchments.
- The MBCn bias correction of the CORDEX dataset improved the hydrological simulations over the catchments, though the performance of CORDEX_MBCn was lower for hydrological variables than for climate variables.
- The timeseries of projected climate changes across the region suggests a gradual increase in temperature, and this led to an increase in potential evaporation (PET). However, the projected changes in precipitation (PRE) are more complex.
- The spatial distribution of the warming is generally consistent across the region, but the magnitude of the warming increases with the GWLs and increases further inland (especially over the north-eastern regions). The spatial distribution of these hydrological changes is consistent with that of PRE.
- The projected decrease in hydrological variables can be linked to the decrease in PRE. There is a decrease in channel precipitation over many areas of the Western Cape, and this drying increases under higher GWLs. The projected increase in PET leads to an increase in stream evaporation, which occurs under all GWLs, and across all the Western Cape catchments, but is enhanced over the Olifants and Gouritz catchments.
- The different land-uses alter the future hydrological water balance. While FOMI increases SW and ET, it decreases runoff (about -0.2 mm mon^{-1}) and increases streamflow (about + 61.9 m^3 s^{-1}). SHRB increases SW and ET but decreases runoff (about -0.2 mm mon^{-1}) and streamflow (about -61.9 m^3 s^{-1}). The hydrological responses of CRDY and GRSL are more complex, as it includes both increases and decreases in hydrological conditions.
- The impacts of FOMI, SHRB, CRDY and GRSL on the hydrological variables and drought are negligible relative to the impact of future climate change.

The results of the study suggest that these land-use changes may not be the most efficient strategies for mitigating the impacts of climate change on hydrological droughts over the Western Cape region. Nevertheless, the local impacts of the land-use changes on hydrological variables are subjective and also likely dependent on the end user upstream/downstream in each catchment area. The approach used in this study only offers insight into the potential hydrological impacts of land-use changes in Western Cape river catchments. It is by no means intended to be prescriptive with regard to regional land-use activities, though it may assist stakeholders and decision makers in making better decisions for land management and water resource planning in a future impacted by drought due to climate change. Further research is required for an improved understanding of the potential for land-use to mitigate drought due to climate change. For instance, it may be that, as ensemble climate change projections (like CORDEX datasets here) improve, SWAT + may better simulate the local hydrology. Future research avenues may also incorporate different drought indices (since indices have different strengths and weaknesses), consider different future emissions trajectories (*e.g.,* a newly built range of the "Shared Socioeconomic Pathways"; SSPs), or consider how other relevant alternative land-use changes (*e.g.,* by the expansion of viticulture) may affect future projections of droughts in the Western Cape.

Supplementary Information The online version contains supplementary material available at https://doi.org/10.1007/s00704-024-04995-7.

Author contributions Both authors designed the study, performed the simulations, and analysed the data. MN drafted the manuscript, and both authors revised it.

Funding Open access funding provided by University of Cape Town. This work was supported with grants from the Water Research Commission (WRC, South Africa) and from the South African Research Chairs Initiative of the Department of Science and Technology and National Research Foundation. The Centre for High Performance Computing (CHPC, South Africa) provided the computing facility used for the study.

Data availability All observational and reanalysis data used in this study are publicly available at no charge and with unrestricted access. The simulation data used in the study are freely available on request.

Declarations

Ethics approval & consent to participate Not applicable.

Consent for publication The authors agreed with the content and gave explicit consent to submit.

Competing interests The authors declare no competing interests.

References

Akoko G, Le TH, Gomi T, Kato T (2021) A review of SWAT model application in Africa. Water 13(9):1313

Albhaisi M, Brendonck L, Batelaan O (2013) Predicted impacts of land use change on groundwater recharge of the upper Berg catchment. South Africa Water SA 39(2):211–220

Andersson JC, Zehnder AJ, Rockström J, Yang H (2011) Potential impacts of water harvesting and ecological sanitation on crop yield, evaporation and river flow regimes in the Thukela River basin. South Africa Agric Water Manag 98(7):1113–1124

Arnold JG, Srinivasan R, Muttiah RS, Williams JR (1998) Large area hydrologic modeling and assessment part I: model development 1. JAWRA J Am Water Resour Assoc 34(1):73–89

Arnold JG, Moriasi DN, Gassman PW, Abbaspour KC, White MJ, Srinivasan R, Santhi C, Harmel RD, Van Griensven A, Van Liew MW (2012) SWAT: Model use, calibration, and validation. Trans ASABE 55(4):1491–1508

BarguésTobella A, Reese H, Almaw A, Bayala J, Malmer A, Laudon H, Ilstedt U (2014) The effect of trees on preferential flow and soil infiltrability in an agroforestry parkland in semiarid Burkina Faso. Water Resour Res 50(4):3342–3354

Bentsen M, Bethke I, Debernard JB, Iversen T, Kirkevåg A, Seland Ø, Drange H, Roelandt C, Seierstad IA, Hoose C, Kristjansson JE (2013) The Norwegian Earth System Model, NorESM1-M–Part 1: description and basic evaluation of the physical climate. Geosci Model Dev 6(3):687–720

Bieger K, Arnold JG, Rathjens H, White MJ, Bosch DD, Allen PM, Volk M, Srinivasan R (2017) Introduction to SWAT+, a completely restructured version of the soil and water assessment tool. JAWRA J Am Water Resour Assoc 53(1):115–130

Botai CM, Botai JO, de Wit JP, Ncongwane KP, Adeola AM (2017) Drought characteristics over the Western Cape Province. South Africa Water 9(11):876

Cannon AJ (2018) Multivariate quantile mapping bias correction: An N-dimensional probability density function transform for climate model simulations of multiple variables. Clim Dyn 50(1):31–49

Cannon AJ, Sobie SR, Murdock TQ (2015) Bias correction of simulated precipitation by quantile mapping: How well do methods preserve relative changes in quantiles and extremes? J Clim 28(17):6938–6959. https://doi.org/10.1175/JCLI-D-14-00754.1

Chylek P, Li J, Dubey MK, Wang M, Lesins GJAC (2011) Observed and model simulated 20th century Arctic temperature variability: Canadian earth system model CanESM2. Atmos Chem Phys Discuss 11(8):22893–22907

Dabrowski JM (2014) Applying SWAT to predict ortho-phosphate loads and trophic status in four reservoirs in the upper Olifants catchment, South Africa. Hydrol Earth Syst Sci Discuss 10(11):2629–2643

Dai A, Zhao T, Chen J (2018) Climate change and drought: A precipitation and evaporation perspective. Curr Climate Chang Rep 4(3):301–312

DEADP (2011) Department of Environmental Affairs and Development Planning. Western Cape (Integrated Water Resource Management) Action Plan: Status Quo Report Final Draft.

Provincial Government, Department of Environmental Affairs and Development Planning. South Africa Chapters 1–13:1–288
Déqué M, Calmanti S, Christensen OB, Aquila AD, Maule CF, Haensler A, Nikulin G, Teichmann C (2017) A multi-model climate response over tropical Africa at +2 °C. Climate Services 7:87–95. https://doi.org/10.1016/J.CLISER.2016.06.002
Dile YT, Daggupati P, George C, Srinivasan R, Arnold J (2016) Introducing a new open-source GIS user interface for the SWAT model. Environ Model Softw 85:129–138
Du Plessis JA, Schloms B (2017) An investigation into the evidence of seasonal rainfall pattern shifts in the Western Cape, South Africa. J South Afr Inst Civil Eng 59(4):47–55
Dufresne JL, Foujols MA, Denvil S, Caubel A, Marti O, Aumont O, Balkanski Y, Bekki S, Bellenger H, Benshila R, Bony S (2013) Climate change projections using the IPSL-CM5 Earth System Model: from CMIP3 to CMIP5. Clim Dyn 40:2123–2165
Dutra E, Viterbo P, Miranda PM (2008) ERA-40 reanalysis hydrological applications in the characterization of regional drought. Geophys Res Lett 35(19):1–5
FAO. Food and Agricultural Organization (2004) Drought impact mitigation and prevention in the limpopo river basin: a situation analysis. Land and water discussion paper. Rome, Italy
Farley KA, Jobbágy EG, Jackson RB (2005) Effects of afforestation on water yield: A global synthesis with implications for policy. Glob Change Biol 11(10):1565–1576
Field CB, Barros VR, Mastrandrea MD, Mach KJ, Abdrabo MK, Adger N, Anokhin YA, Anisimov OA, Arent DJ, Barnett J, Burkett VR (2014) Summary for policymakers. In Climate change 2014: impacts, adaptation, and vulnerability. Part A: global and sectoral aspects. Contribution of Working Group II to the Fifth Assessment Report of the Intergovernmental Panel on Climate Change (pp 1–32). Cambridge University Press
Flörke M, Schneider C, McDonald RI (2018) Water competition between cities and agriculture driven by climate change and urban growth. Nature Sustain 1(1):51–58
Green Cape (2019) Sustainable Agriculture 2019 Market Intelligence Report. Cape Town, South Africa. Available online: http://www.greencape.co.za.
Giorgi F, Jones C, Asrar GR (2009) Addressing climate information needs at the regional level: the CORDEX framework. World Meteorol Org (WMO) Bulletin, 58(3), pp 175–183
Gordon HB, Rotstayn LD, McGregor JL, Dix MR, Kowalczyk EA, O'farrell SP, Waterman LJ, Hirst AC, Wilson SG, Collier MA, Watterson IG (2002) The CSIRO Mk3 climate system model
Gropp W, Lusk E, Doss N, Skjellum A (1996) A high-performance, portable implementation of the MPI message passing interface standard. Parallel Comp 22:828
Guo JT, Zhang ZQ, Wang SP, Strauss P, Yao AK (2014) Appling SWAT model to explore the impact of changes in land-use and climate on the streamflow in a Watershed of Northern China. Acta Ecol Sin 34(6):1559–1567
Gyamfi C, Ndambuki JM, Salim RW (2016a) Hydrological Responses to Land-use/Cover Changes in the Olifants Basin. South Afr Water 8(12):588
Gyamfi C, Ndambuki JM, Salim RW (2016b) Simulation of sediment yield in a semi-arid river basin under changing land use: an integrated approach of hydrologic modelling and principal component analysis. Sustainability 8(11):1133
Haensler A, Hagemann S, Jacob D (2011) Dynamical downscaling of ERA40 reanalysis data over southern Africa: added value in the simulation of the seasonal rainfall characteristics. Int J Climatol 31(15):2338–2349. https://doi.org/10.1002/joc.2242
Herold CE, Bailey AK (2016) Water Resources of South Africa Study (WR2012). River Streamflow Gauging and Reservoir Inflow Database. Available online: https://waterresourceswr2012.co.za/. Accessed 17 Aug 2021
Holder AJ, Rowe R, McNamara NP, Donnison IS, McCalmont JP (2019) Soil & Water Assessment Tool (SWAT) simulated hydrological impacts of land-use change from temperate grassland to energy crops: A case study in the western UK. GCB Bioenergy 11(11):1298–1317
Jarvis A, Reuter HI, Nelson A, Guevara E (2008) Hole-filled SRTM for the globe Version 4, available from the CGIAR-CSI SRTM 90m Database. https://srtm.csi.cgiar.org
Jia X, Zhu Y, Luo Y (2017) Soil moisture decline due to afforestation across the Loess Plateau, China. J Hydrol 546:113–122
Jury MR (2018) The climate of desiccation in the SW Cape. Hydrology and earth system sciences discussions, pp 1–19
Kotzé I, Beukes H, Van den Berg E, Newby T (2010) National invasive alien plant survey. Report number: gw/a/2010/21, pp 1–55
Krysanova V, White M (2015) Advances in water resources assessment with SWAT—an overview. Hydrol Sci J 60(5):771–783
Lakhraj-Govender R, Grab SW (2019) Rainfall and river flow trends for the Western Cape Province, South Africa. S Afr J Sci 115(9–10):1–6
Le Maitre DC, Versfeld DB, Chapman RA (2000) Impact of invading alien plants on surface water resources in South Africa: a preliminary assessment. Water SA 26(3):1–12
Le Maitre DC, Forsyth GG, Dzikiti S, Gush MB (2016) Estimates of the impacts of invasive alien plants on water flows in South Africa. Water SA 42(4):659–672
Le Maitre D, Görgens A, Howard G, Walker N (2019) Impacts of alien plant invasions on water resources and yields from the Western Cape Water Supply System (WCWSS). Water SA 45(4):568–579
Lechmere-Oertel RG (1998) The environmental determinants of the Fynbos/succulent karoo boundary in Matjiesrivier Nature Reserve, Western Cape (Master's thesis, University of Cape Town)
Louw EJM (2007) Climate change in the western cape: a disaster risk assessment of the impact on human health. Doctoral dissertation. University of Stellenbosch
Lumsden TG, Schulze RE (2003) Modelling the impacts of land cover and land management practices on stream flow reduction. Pretoria: water research commission
Luo J, Zhou X, Rubinato M, Li G, Tian Y, Zhou J (2020) Impact of multiple vegetation covers on surface runoff and sediment yield in the small basin of Nverzhai, Hunan Province. China Forests 11(3):329
Mahlalela PT, Blamey RC, Reason CJC (2019) Mechanisms behind early winter rainfall variability in the southwestern Cape. South Afr Clim Dyn 53(1):21–39
Marais D, Fischer T, Kotze D, Haasbroek B, Govender M, Pugin J, Horn A (2021) Economic valuation of the averted degradation of the Vyeboom Wetland in the Theewaterskloof Dam catchment. South Afr Water SA 47(1):24–34
Mbokodo I, Bopape M-J, Chikoore H, Engelbrecht F, Nethengwe N (2020) Heatwaves in the future warmer climate of South Africa. Atmosphere (basel) 11(7):712
McKee TB, Doesken NJ, Kleist J (1993) The relationship of drought frequency and duration to timescales. In: Proceedings of the 8th conference on applied climatology. Am Meteorol Soc, pp 179–183
Mengistu AG, van Rensburg LD, Woyessa YE (2019) Techniques for calibration and validation of SWAT model in data scarce arid and semi-arid catchments in South Africa. J Hydrol: Reg Stud 25:100621
Midgley GF, Chapman RA, Hewitson B, Johnston P, De Wit M, Ziervogel G, Mukheibir P, Van Niekerk L, Tadross M, Van Wilgen BW, Kgope B (2005) A status quo, vulnerability and adaptation assessment of the physical and socio-economic effects of climate change in the Western Cape. Report to the Western Cape Government, Cape Town, South Africa. CSIR Report No. ENV-S-C 2005–073, Stellenbosch, pp 1–171

Midgley G, Chapman R, Mukheibir P, Tadross M, Hewitson B, Wand S, Schulze R, Lumsden T, Horan M, Warburton M, Kgope B (2007) Impacts, vulnerability, and adaptation in key South African sectors: an input into the long-term mitigation scenarios process

Moriasi DN, Arnold JG, Van Liew MW, Bingner RL, Harmel RD, Veith TL (2007) Model evaluation guidelines for systematic quantification of accuracy in watershed simulations. Transactions of the ASABE 50(3):885–900

Moriasi DN, Gitau MW, Pai N, Daggupati P (2015) Hydrologic and water quality models: performance measures and evaluation criteria. Transactions of the ASABE 58(6):1763–1785

Naik M, Abiodun BJ (2016) Potential impacts of forestation on future climate change in Southern Africa. Int J Climatol 36(14):4560–4576. https://doi.org/10.1002/joc.4652

Naik M, Abiodun BJ (2020) Projected changes in drought characteristics over the Western Cape. South Afr Meteorol Appl 27(1):e1802

Ncube M, Taigbenu AE (2005) The impact of land cover and land use on hydrological response in the Olifants Catchment. In: Proceedings of special colloquium water research showcase, Universities of Johannesburg, Pretoria and the Witwatersrand, pp 51–54

NDMC (2021) National drought mitigation centre. School of natural resources. Available online: https://drought.unl.edu/. Accessed 17 Aug 2021

Neitsch SL Arnold JG, Srinivasan R (2002) Pesticide's fate and transport predicted by the soil and water assessment tool (SWAT). Atrazine, Metolachlor Trifluralin Sugar Creek Watershed: BRC Report, 3

Nikulin G, Lennard C, Dosio A, Kjellström E, Chen Y, Hänsler A, Kupiainen M, Laprise R, Mariotti L, Maule CF, van Meijgaard E, Panitz H-J, Scinocca JF, Somot S (2018) The effects of 1.5 and 2 degrees of global warming on Africa in the CORDEX ensemble. Environ Res Lett 13(6):065003

Popke D, Stevens B, Voigt A (2013) Climate and climate change in a radiative-convective equilibrium version of ECHAM6. J Adv Model Earth Syst 5(1):1–14

Refsgaard JC (1997) Parameterisation, calibration and validation of distributed hydrological models. J Hydrol 198(1–4):69–97

Riahi K, Rao S, Krey V, Cho C, Chirkov V, Fischer G, Kindermann G, Nakicenovic N, Rafaj P (2011) RCP 8.5 – A scenario of comparatively high greenhouse gas emissions. Clim Change 109:33–57

Rostorfer D, Mitler D, Ledbetter K (2015) Creating shared value through corporate social investment: managing water-related risk and opportunity through coca-cola's replenish Africa initiative. Master of Science Thesis in Natural Resources and Environment at the University of Michigan, pp 1–328

Roux (2018) Agricultural water file: farming for a drier future. WWF South Africa

Samuelsson P, Gollvik S, Kupiainen M, Kourzeneva E van de Berg WJ (2015) The surface processes of the Rossby Centre regional atmospheric climate model (RCA4). SMHI

Schütte S, Schulze RE (2017) Projected impacts of urbanisation on hydrological resource flows: A case study within the uMngeni Catchment, South Africa. J Environ Manage 196:527–543

Scott-Shaw BC, Hill TR, Gillham JS (2020) Calibration of a modelling approach for sediment yield in a wattle plantation, KwaZulu-Natal. South Afr Water SA 46(2):171–181

Sheffield J, Goteti G, Wen F, Wood EF (2004) A simulated soil moisture-based drought analysis for the United States. J Geophys Res: Atmos 109(D24):1–19

Sheffield J, Goteti G, Wood EF (2006) Development of a 50-year high-resolution global dataset of meteorological forcings for land surface modeling. J Clim 19(13):3088–3111

Shukla S, Wood AW (2008) Use of a standardized runoff index for characterizing hydrologic drought. Geophys Res Lett 35(2):1–7

Sousa PM, Blamey RC, Reason CJ, Ramos AM, Trigo RM (2018) The 'Day Zero' Cape Town drought and the poleward migration of moisture corridors. Environ Res Lett 13(12):124025

Tan ML, Gassman PW, Srinivasan R, Arnold JG, Yang X (2019) A review of SWAT studies in Southeast Asia: applications, challenges and future directions. Water 11(5):914

Tarboton DG (1997) A new method for the determination of flow directions and upslope areas in grid digital elevation models. Water Resource Research 33:309

Taylor KE, Stouffer RJ, Meehl GA (2012) An overview of CMIP5 and the experiment design. Bull Am Meteor Soc 93(4):485–498

Thavhana MP, Savage MJ, Moeletsi ME (2018) SWAT model uncertainty analysis, calibration and validation for runoff simulation in the Luvuvhu River catchment, South Africa. Phys Chem Earth, Parts a/b/c 105:115–124

Tizora P, Le Roux A, Mans GG, Cooper AK (2016) Land-use and land cover change in the Western Cape Province: Quantification of changes and understanding of driving factors. Available online: https://www.researchspace.csir.co.za.

Turpie J (2018) Clearing thirsty alien trees will yield water returns for Cape Town. Dly. Maverick. https://www.dailymaverick.co.za/article/2018-07-02-clearing-thirsty-alien-trees-willyieldwater-returns-for-cape-town/. Accessed 30 Jan 2019.

Ground Up (2018) Aliens are the greatest threat to Cape Town's water security. Ground Up. Available online: http://www.groundup.org.za.

Van Niekerk A, Joubert SJ (2011) Input variable selection for interpolating high-resolution climate surfaces for the Western Cape. Water SA 37(3):1–10

Van Griensven A, Ndomba P, Yalew S, Kilonzo F (2012) Critical review of SWAT applications in the upper Nile basin countries. Hydrol Earth Syst Sci 16(9):3371–3381

Vicente-Serrano SM, Beguería S, López-Moreno JI (2010) A multiscalar drought index sensitive to global warming: the standardized precipitation evapotranspiration index. J Clim 23(7):1696–1718

Voldoire A, Sanchez-Gomez E, Salas y Mélia D, Decharme B, Cassou C, Sénési S, Valcke S, Beau I, Alias A, Chevallier M, Déqué M (2013) The CNRM-CM5. 1 global climate model: description and basic evaluation. Clim Dyn 40:2091–2121

Warburton ML, Schulze RE, Jewitt GP (2012) Hydrological impacts of land use change in three diverse South African catchments. J Hydrol 414:118–135

Watanabe S, Hajima T, Sudo K, Nagashima T, Takemura T, Okajima H, Nozawa T, Kawase H, Abe M, Yokohata TJGMD, Ise T (2011) MIROC-ESM 2010: Model description and basic results of CMIP5-20c3m experiments. Geoscie Model Dev 4(4):845–872

Welderufael WA, Woyessa YE, Edossa DC (2013) Impact of rainwater harvesting on water resources of the modder river basin, central region of South Africa. Agric Water Manag 116:218–227

Wilhite DA (2005) Drought and water crises: Science, technology, and management issues. CRC Press

Yen H, Park S, Arnold JG, Srinivasan R, Chawanda CJ, Wang R, Feng Q, Wu J, Miao C, Bieger K, Daggupati P (2019) IPEAT+: A Built-in optimization and automatic calibration tool of SWAT+. Water 11(8):1681

Youpeng X, Jintao X, Jinjia D, Ying C, Yixing Y, Xingqi Z (2010) Impacts of urbanization on hydrology in the Yangtze River Delta. China Water Science and Technology 62(6):1221–1229

Yuan X, Bai J (2018) Future projected changes in local evapotranspiration coupled with temperature and precipitation variation. Sustainability 10(9):3281